DEUTSCHES ELEKTRONEN-SYNCHROTRON DESY

DESY 80/85
September 1980

JETS IN e^+e^- ANNIHILATION AT HIGH ENERGIES

by

Günter Wolf

NOTKESTRASSE 85 · 2 HAMBURG 52

To be sure that your preprints are promptly included in the
HIGH ENERGY PHYSICS INDEX ,
send them to the following address (if possible by air mail) :

DESY
Bibliothek
Notkestrasse 85
2 Hamburg 52
Germany

DESY 80/85
September 1980

Jets in e^+e^- Annihilation at High Energies(*)

Günter Wolf
DESY, Hamburg

1. Introduction

Hadrons produced in e^+e^- annihilation are emitted into two back-to-back cones which become narrower as the c.m. energy increases. This two-jet structure was first observed in 1975 by the SLAC-LBL group[1] studying charged particles produced in e^+e^- collisions between 3.0 and 7.4 GeV at SPEAR. Subsequent experiments done in 1978 by the PLUTO group[2] at DORIS confirmed this behaviour and extended the measurements up to 10 GeV c.m. energy. In the latter experiments also the neutral component was analyzed and the jet axis of the neutral component was found to coincide with the axis determined with charged particles.

A marked deviation from two-jet production was observed at the position of the Υ by several DORIS experiments[3-5]. The analysis presented by the PLUTO group[6] strongly suggested that the direct decays of the Υ proceed via a three-gluon intermediate state leading to three hadronic jets in the final state[7]. Furthermore, the data preferred spin one for the gluons[8].

The commissioning of PETRA in 1978 opened the possibility to push the e^+e^- experiments to much higher energies. Studying nonresonant hadron production at energies around 30 GeV in 1979 the TASSO group[9] found a new process which leads to three-jet events. This observation was confirmed by the MARK J[10], PLUTO[11] and JADE[12] groups working also at PETRA. The properties of the

* Talk given at the XI International Symposium on Multiparticle Dynamics, Bruges, Belgium, June 22-27, 1980

three jet events matched well the warrant given by theorists for hard gluon bremsstrahlung[13].

A careful study of particle distributions between jet axes made by JADE suggests a difference between quark and gluon fragmentation. Two particle angular correlations measured by PLUTO indicate the importance of multiple and soft gluon emission for near back-to-back jets.

This report will review the experimental knowledge of jet formation in e^+e^- annihilation at high energies. Apart from the published material more information can be found in recent reviews[14,15].

2. Jet formation in the quark model

The quark model views e^+e^- annihilation into hadrons as a two step process (see Fig. 1); first a pair of quarks is produced (a) which then fragment into hadrons (b).

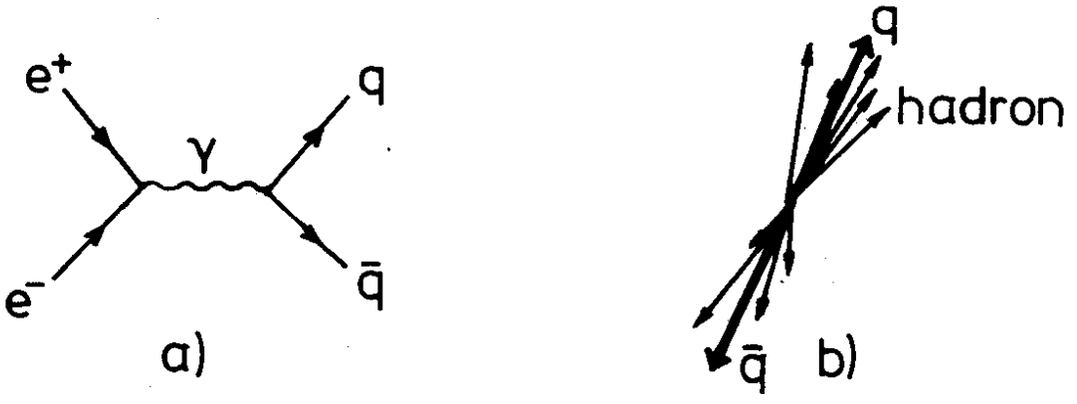

Fig. 1 e^+e^- annihilation in the quark model

The occurence of jets is natural in this model. If the hadron momenta transverse to the quark direction of flight are limited and the number of produced hadrons grows only slowly with energy, the emitted hadrons will be more and more collimated around the primary quark direction as the total energy increases. Let W be the total c.m. energy, $\langle n \rangle$ be the average particle multiplicity, $\langle P_T \rangle$ and $\langle P_{||} \rangle \sim \langle P \rangle \sim W/\langle n \rangle$ the average transverse and longitudnal hadron momenta, then the mean half angle $\langle \delta \rangle$ of the jet cones can be estimated:

$$\langle \delta \rangle = \left\langle \frac{P_T}{P_{||}} \right\rangle \approx \frac{\langle P_T \rangle \cdot \langle n \rangle}{W} \sim \frac{1}{W} \qquad (1)$$

The jet cones shrink roughly $\sim W^{-1}$. (Actually, in a realistic calculation of the quark model using the fragmentation functions of Field and Feynman[16] one finds $\langle \delta \rangle \sim W^{-1/2}$).

This simple picture of e^+e^- annihilation into hadrons is strongly supported by the data. Besides the jet structure of the events important tests in favour of the quark model are provided by the angular distribution of the jet axis and the size and energy dependence of the total cross section.

The angular distribution of the jet axis with respect to the beam direction was found to be of the form[1]

$$W(\cos\Theta) \sim 1 + \cos^2\Theta$$

which is what is expected if the primary partons have spin 1/2. For comparison, partons with spin zero would lead to $W \sim 1 - \cos^2\Theta$.

The total cross section is readily calculated. The cross section for producing a free $q\bar{q}$ pair is the same as for producing a $\mu^+\mu^-$ pair ($\sigma_{\mu\mu} = \frac{4\pi}{3}\frac{\alpha}{W^2}$) except that the quark charge e_q replaces the muon charge 1. Assuming that the produced $q\bar{q}$ pair turns into hadrons with unit probability the total cross section with respect to $\sigma_{\mu\mu}$ is found by summing the square of the quark charges,

$$R \equiv \sigma(e^+e^- \to \text{hadrons})/\sigma_{\mu\mu} = 3 \sum_{q=u,d,\ldots} e_q^2 \qquad (2)$$

where the factor 3 is the colour factor.

Fig. 2 summarizes the R measurements. The outstanding features of R are the spikes due to the excitation of vector states ($\rho,\omega,\ldots$) and the fact that in between the families of vector states ($\rho\ldots$, $J/\psi\ldots$, $\Upsilon\ldots$) R is almost constant. The quark model, prediction (2), is in striking agreement (to within 30 %) with the data. Up to 3 GeV only u,d and s contribute and therefore R = 2. Above charm threshold (near 4 GeV) R should rise to a level of 3.3. Beyond the Υ family in addition the b quark contribution has to be included raising R to 3.7 in accord with the data.

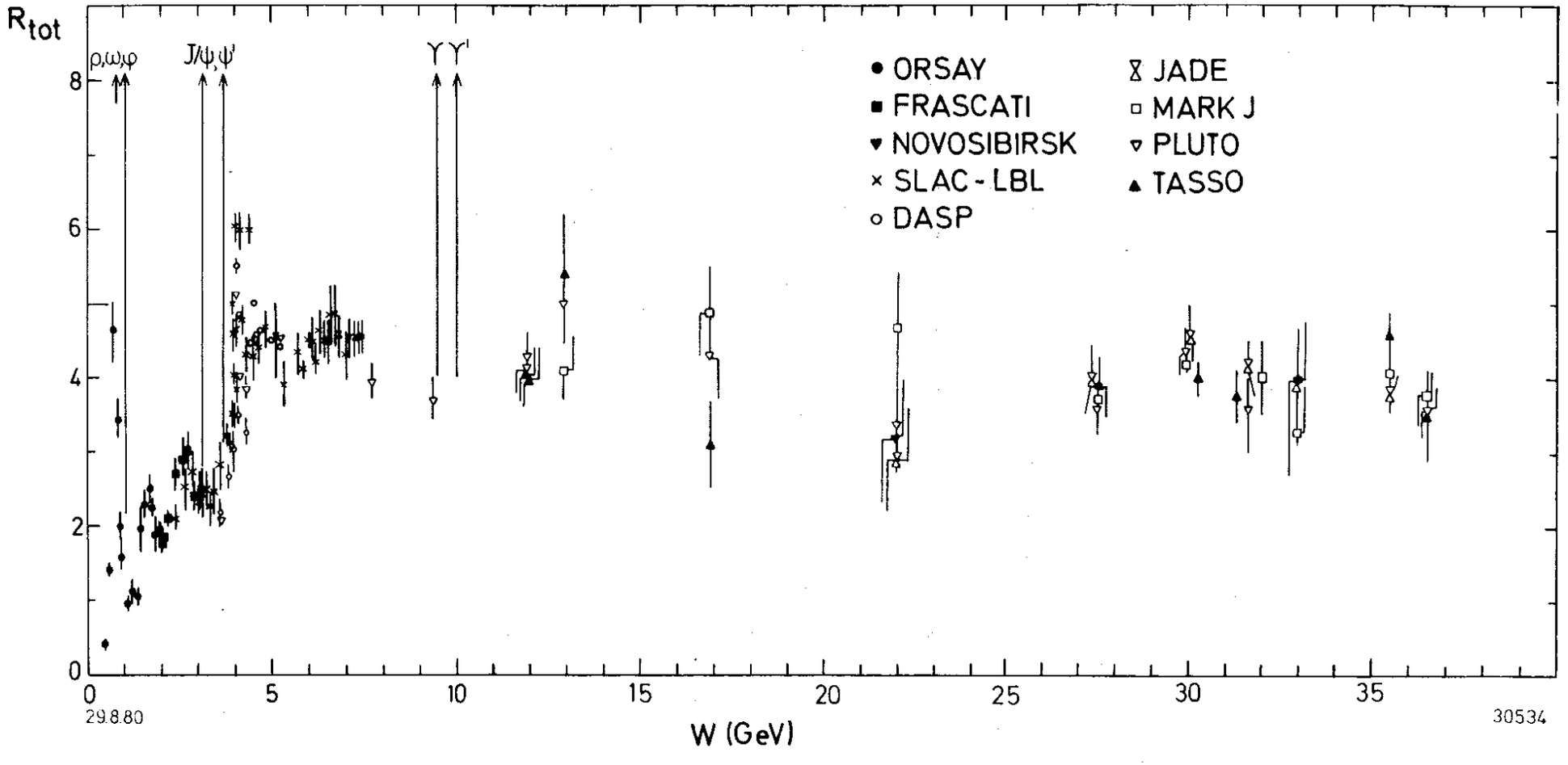

Fig. 2 The ratio R of the total hadronic cross section to $\sigma_{\mu\mu} = \frac{4\pi\alpha^2}{3s}$ as a function of the c.m. energy (from Ref.17)

3. Jet measures

The jet axis and the amount of collimation is commonly determined in terms of sphericity[19], S and thrust[20], T;

$$S = 3/2 \quad (\sum P_{Ti}^2)/(\sum P_i^2) \; ; \qquad T = \sum |P_{\parallel i}| / \sum P_i \qquad (3)$$

$$0 \leq S \leq 1 \qquad\qquad 0.5 \leq T \leq 1$$

where P_{Ti}, $P_{\parallel i}$ are the transverse and longitudinal momenta relative to the jet axis which is chosen such that $\sum P_{Ti}^2$ ($\sum |P_{\parallel i}|$) is minimal (maximal) for sphericity (thrust). Sphericity measures approximately the square of the jet cone half opening angle

$$S \approx 3/2 \; \langle \delta^2 \rangle$$

and likewise $T \approx \sqrt{1 - \langle \delta \rangle^2}$.

Extreme jettiness ($\delta = 0$) leads to $S = 0$ and $T = 1$ while for spherical events $S \to 1$ and $T \to 0.5$.

4. Two-jet production

Fig. 3 shows the energy dependence of the average sphericity as measured at DORIS and PETRA. At low energies, $W \lesssim 4$ GeV, the observed $\langle S \rangle$ values are close to those predicted by phase space, $\langle S \rangle \approx 0.4$. Above 5 GeV $\langle S \rangle$ decreases rapidly with increasing W i.e. the particles become more and more collimated in clear distinction to a phase space behaviour. A power law, $\langle S \rangle = 0.8 \; W^{-1/2}$ describes the data well. The jet cone half opening angle as inferred from $\langle S \rangle$ shrinks from $\sim 31^\circ$ at W = 4 GeV to 17° near 36 GeV. Fig.4 shows the sphericity distribution measured near 30 GeV. The strong preference for small S values is clearly seen. 80% of the events have $S < 0.25$ or $\langle \delta \rangle \simeq 23^\circ$. An analysis of the data in terms of thrust leads to the same conclusions (see Fig.5).

Despite the narrowness of the jet cone the spread of the particles around the jet axis is appreciable, in particular of the low energetic ones. This is illustrated by Fig.6 which shows the fraction of energy f for charged plus neutrals observed outside a jet cone with half opening angle δ. The measurement was done by PLUTO at W=9.4 GeV, where $\langle \delta \rangle \simeq 24^\circ$. The energy flow around the jet axis has a long tail reaching out to the limit ($\delta = 90^\circ$).

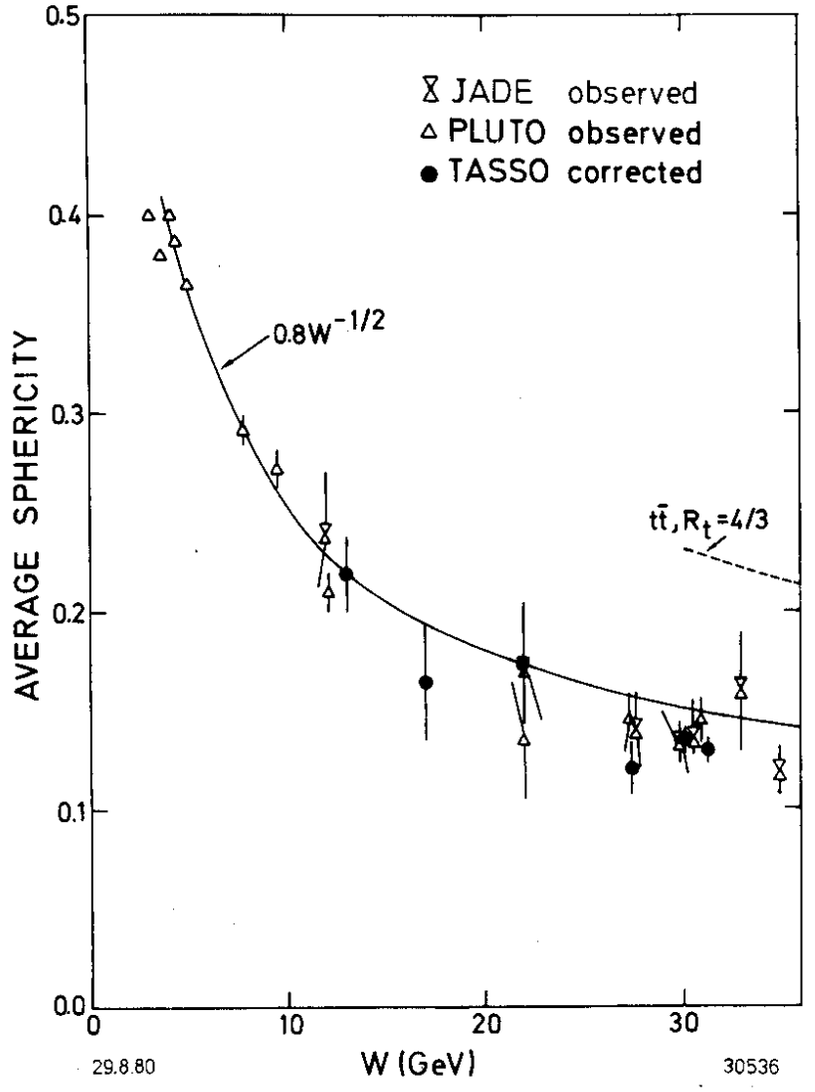

Fig. 3 The average sphericity as a function of the c.m. energy.

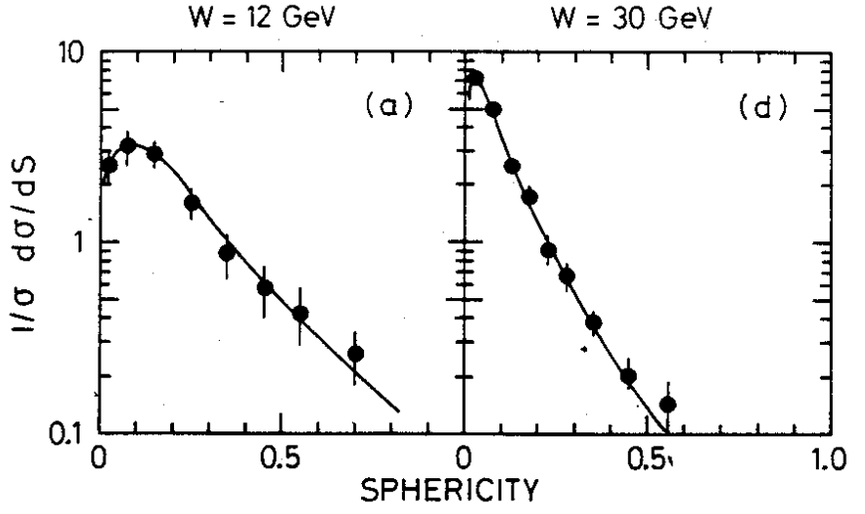

Fig. 4 Sphericity distributions measured at W=12 and 30 GeV (Ref. 37)

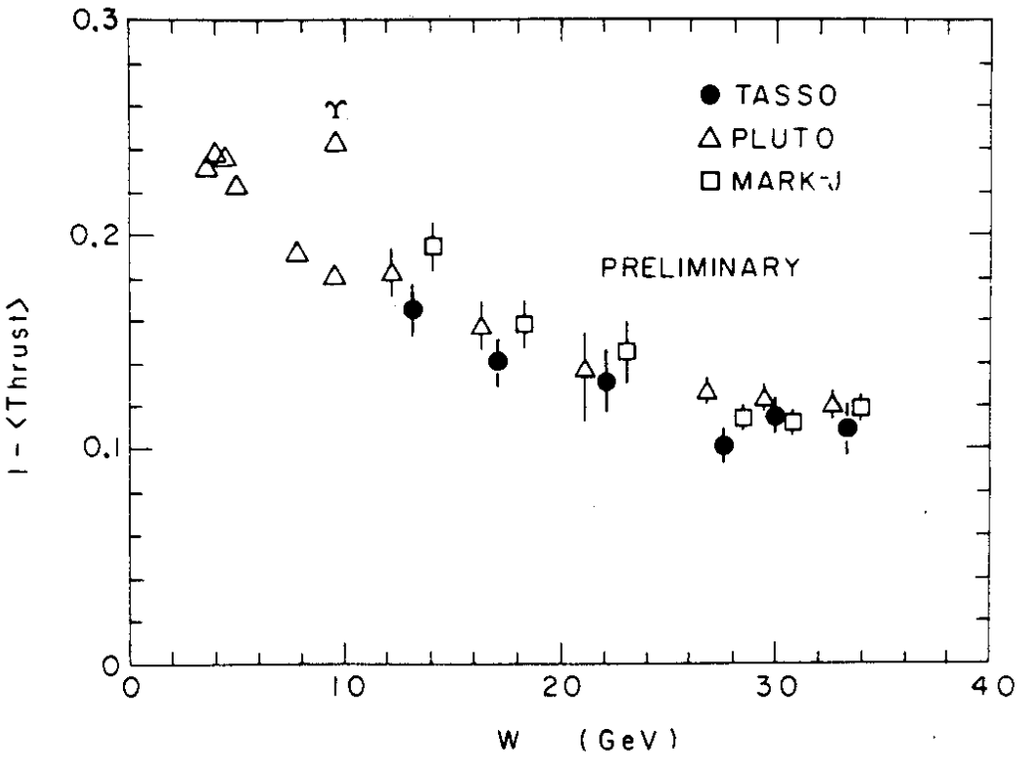

Fig. 5 The average of 1 - thrust as a function of the c.m. energy

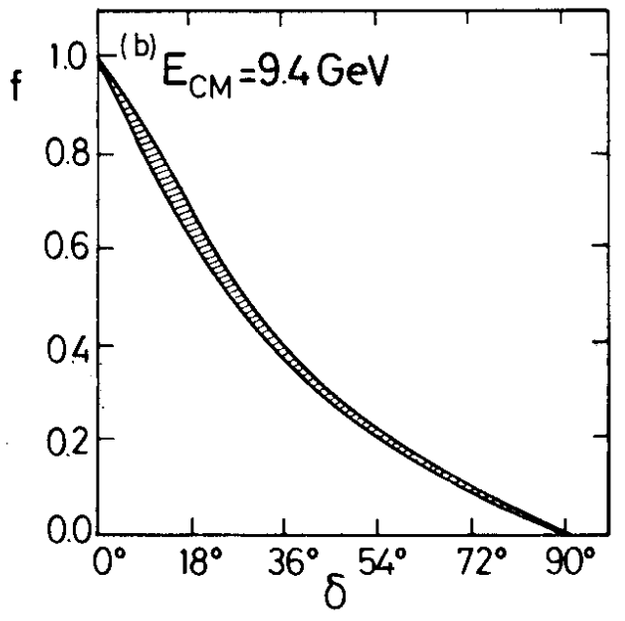

Fig.6 The average fraction of visible energy (f) outside a cone of half angle δ at 9.4 GeV (Ref. 21).

5. Transverse momentum distributions and jet broadening

The transverse momentum distribution of hadrons produced in hadron scattering suggested a Gaussian p_T distribution for quark fragmentation into hadrons:

$$\frac{d\sigma}{dp_T^2} \sim e^{-\frac{p_T^2}{2\sigma q^2}} \qquad (4)$$

The parameter σ_q e.g. for pions was found to be of the order of 250 MeV/c almost independent of the reaction energy. Deviations from a simple Gaussian behavior - a flattening of the p_T distribution - were observed in pp collisions at high p_T values[23]. The e^+e^- annihilation data at energies up to 7.4 GeV were found to be consistent with an energy independent σ_q around 300 MeV/c [1]. However, when comparing data taken at 13, 17 GeV with those near 30 GeV the TASSO group found a large broadening of the p_T distribution with increasing energy[9]. The broadening was correlated with the appearance of planar events, some of which had a definite three jet structure. The properties of these events as well as their production rate agreed well with the predictions for gluon bremsstrahlung by Ellis, Gaillard and Ross[13].

We now discuss the experimental evidence for three jet events. Fig. 7 shows the normalized transverse momentum distribution $1/\sigma_{tot}\ d\sigma/dp_T^2$ evaluated with respect to the sphericity axis for 12, 13 - 17 and 27 - 32 and 35 - 36 GeV as measured by TASSO. The measurements for the three energies are in reasonable agreement for $p_T^2 < 0.2\ (GeV/c)^2$, but the high energy data are well above the low energy data for larger values of p_T^2 in contradiction to the naive parton model which assumes the quark to fragment with an energy independent transverse momentum distribution. The low energy data were fitted for $p_T^2 < 1\ (GeV/c)^2$ with the $q\bar{q}$ model[16] including c and b quarks[24]. Increasing the parameter σ_q (eq.11.9) from its original value of 0.25 GeV/c to 0.30 GeV/c gave a good fit to the 12 and 13 - 17 GeV data. To fit the higher energy data with the same model σ_q had to be increased to 0.45 GeV/c. Fig. 8 shows the average p_T^2 as a function of W: it is seen to rise rapidly for $W \gtrsim 12$ GeV.

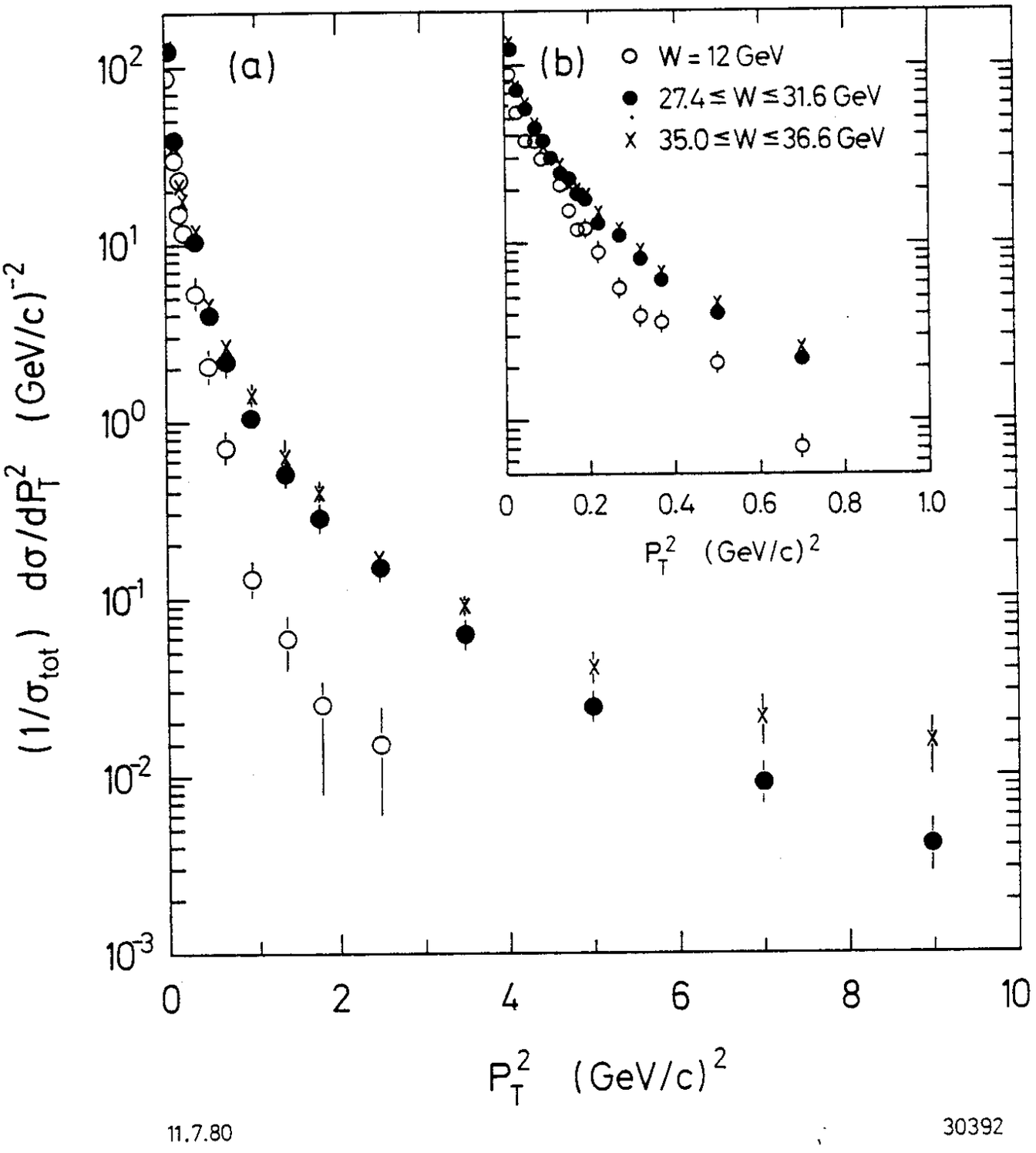

Fig. 7 The p_T^2 distribution as measured by TASSO at c.m. energies of 12, 27.4 - 31.6 and 35.0 - 36.6 GeV.

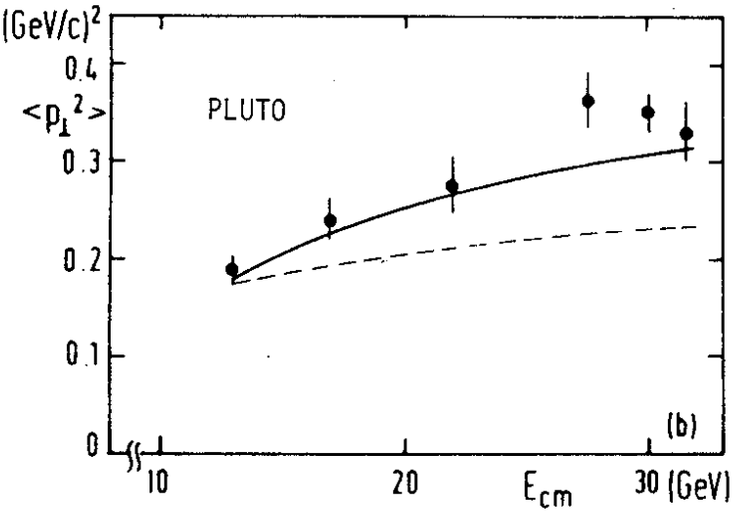

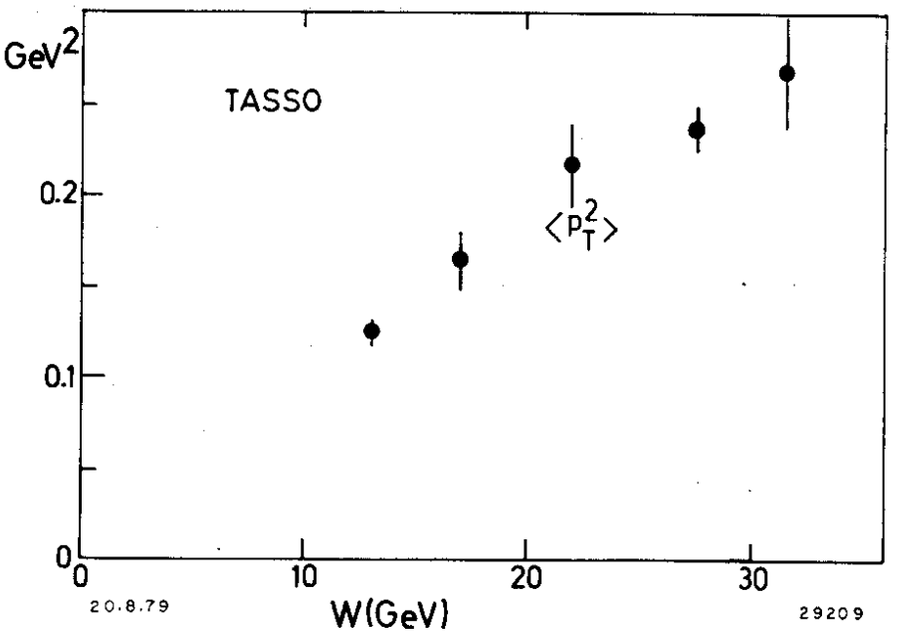

Fig. 8 The average of the transverse momentum squared as a function of the c.m. energy measured by PLUTO and TASSO.

The widening of the transverse momentum distribution can have different origins:

1. the production of a new quark flavor. The data do not show any evidence for the production of a new heavy quark and we can dismiss that as a possible explanation.

2. the p_T distribution for quark fragmentation into hadrons is energy dependent: the average p_T grows as the energy increases. In this case the hadrons are still produced in two jets but the diameter of the "cigar" in terms of p_T^2 increases with energy (see sketch). Note also that both jets will grow in the same manner.

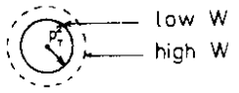

3. gluon bremsstrahlung from the outgoing quarks[13].

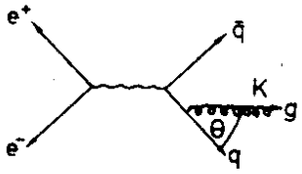

Schematic diagram for gluon emission

The radiated gluon carrying colour will turn into a jet of hadrons. The energy and angular distribution of the gluon is similar to that of a photon emitted by an electron.

Denoting by x_1, x_2 the fractional energies of the quarks, $x_i = 2E_i/W$, the cross section for gluon emission is given by

$$\frac{d\sigma(q\bar{q}g)}{dx_1\,dx_2} = \frac{2\alpha_s}{3\pi}\,\sigma_o\,\frac{x_1^2 + x_2^2}{(1-x_1)(1-x_2)} \qquad (5)$$

where σ_o is the parton model cross section for quark pair production, $\sigma_o = 3\sigma_{\mu\mu}\sum e_q^2$, and α_s is the strong (running) coupling constant,

$$\alpha_s(s) = \frac{12\pi}{(33-2N_f)\ln s/\Lambda^2} \qquad (6)$$

N_f = number of flavours (= 5 for u,d,...b)
$s = W^2$
Λ a constant

A crude approximation of eq(5) yields for small θ, K

$$\frac{d\sigma(q\bar{q}g)}{dK\, d\theta} \sim \frac{\alpha_s}{K \sin\theta}\, \sigma_o \qquad (7)$$

where K is the energy and θ the production angle of the gluon measured with respect to the quark. The average transverse momentum of the (hard) gluon jet is

$$\langle K_T \rangle \sim \frac{\alpha_s \cdot \sigma_o \iint \frac{K \sin\theta}{K \sin\theta}\, dK d\theta}{\sigma_o \left(1 + \frac{\alpha_s}{\pi}\right)}$$

$$\sim \alpha_s \cdot W \quad \text{(up to log terms)}$$

(For the total cross section the first order QCD result, $\sigma_{tot} = \sigma_o \left(1 + \frac{\alpha_s}{\pi}\right)$ was inserted). The remarkable result is that contrary to many other predictions of QCD which lead to logarithmic deviations from the pure quark model and are therefore difficult to test experimentally, the transverse momentum is predicted to rise linearly with energy. If K_T is large compared to the typical transverse momentum of 0.3 GeV/c, then the event will have a three jet topology.

Detection of the gluon jet requires high c.m. energies for two reasons. Firstly, at low energies gluon and quark jets are broad and will overlap. Secondly, at low energies where $\alpha_s(s)$ is of order one, single as well as multigluon emission is important, and besides, perturbative QCD may not be applicable. The additional gluon jets aggravate the overlap problem at low energies. However, as the energy goes up the jets become narrower and $\alpha_s(s)$ becomes smaller; e.g. at the highest PETRA energies, $s \approx 1000\ GeV^2$, $\alpha_s(s)$ is around 0.2 such that the emission of several hard gluons can be neglected.

6. Planar events

The event shapes were studied by TASSO, PLUTO and JADE using the momentum tensor ellipsoid and by MARK J determining the oblateness.

Momentum tensor ellipsoid

For each event one constructs the second rank tensor from the hadron momenta[19]

$$M_{\alpha\beta} = \sum_{j=i}^{N} P_{j\alpha} P_{j\beta} \quad (\alpha,\beta = x, y, z) \tag{8}$$

summing over all N observed charged particles. Let $\hat{n}_1$, $\hat{n}_2$ and $\hat{n}_3$ be the unit eigenvectors of this tensor associated with the eigenvalues Λ_1, Λ_2 and Λ_3 which are ordered such that $\Lambda_1 < \Lambda_2 < \Lambda_3$. Note that

$$\Lambda_i = \sum(\vec{p}_j \hat{n}_i)^2 \tag{9}$$

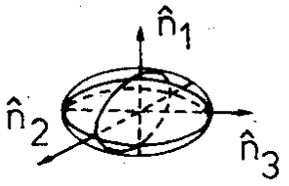

The principal axis is the $\hat{n}_3$ direction which is identical to the jet axis determined by sphericity; the event plane is the $\hat{n}_2$, $\hat{n}_3$ plane and $\hat{n}_1$ defines the direction in which the sum of the square of the momentum components is minimal.

Define the normalized eigenvalues

$$Q_i = \frac{\Lambda_i}{\Sigma p_j^2} = \frac{\Sigma(\vec{p}_j \cdot \hat{n}_i)^2}{\Sigma p_j^2} \tag{10}$$

which satisfy the relation

$$Q_1 + Q_2 + Q_3 = 1$$

Generally speaking the Q_i measure the

flatness (Q_1)
width (Q_2)
length (Q_3)

of an event.

The events will be characterized by the two variables aplanarity A and sphericity S

$$A = \frac{3}{2} Q_1$$

$$S = \frac{3}{2} (Q_1 + Q_2) = \frac{3}{2} (1 - Q_3) \qquad (11)$$

Since $0 < Q_1 < Q_2 < Q_3 < 1$ all events lie inside a triangle.

Planar events

In Figs. 9-11 the distributions of

$$\langle p^2_{Tout} \rangle = \frac{1}{N} \sum_{j=1}^{N} (\vec{p}_j \cdot \hat{n}_1)^2 \quad (= Q_1 \Sigma p_j^2) \qquad (12)$$

(= square of the momentum component normal to the event plane given by $\hat{n}_2$ and $\hat{n}_3$) are compared with that of

$$\langle p^2_{Tin} \rangle = \frac{1}{N} \sum_{j=1}^{N} (\vec{p}_j \cdot \hat{n}_2)^2 \quad (= Q_2 \Sigma p_j^2) \qquad (13)$$

(= square of the momentum component in the event plane perpendicular to the jet axis). The data from TASSO[25], PLUTO[26] and JADE[27] show little increase in $\langle p^2_{Tout} \rangle$ from low to high energy data. The distribution of $\langle p^2_{Tin} \rangle$, however, becomes much wider at high energies; in particular there is a long tail of events with high $\langle p^2_{Tin} \rangle$. The predictions of the $q\bar{q}$ model are also shown. Hadrons resulting from pure $q\bar{q}$ jets will on the average be distributed uniformly around the jet axis. However, some asymmetry between $\langle p^2_{Tout} \rangle$ and $\langle p^2_{Tin} \rangle$ is caused by statistical fluctuations. Fair agreement with the $q\bar{q}$ model is found at the low energy point. Thus the asymmetry observed at this energy can be explained by statistical fluctuations alone.

At high energy, one finds fair agreement for $\langle p^2_{Tout} \rangle$ with the $q\bar{q}$ model with $\sigma_q \approx 0.3$ GeV/c, however, the long tail of the $\langle p^2_{Tin} \rangle$ distribution is not reproduced by the model. This discrepancy cannot be removed by increasing σ_q. The result with $\sigma_q = 0.45$ GeV/c is also plotted in Fig. 9. The agreement is poor. One therefore must conclude that the data include a number of planar events that are not reproduced by the $q\bar{q}$ model independent of the

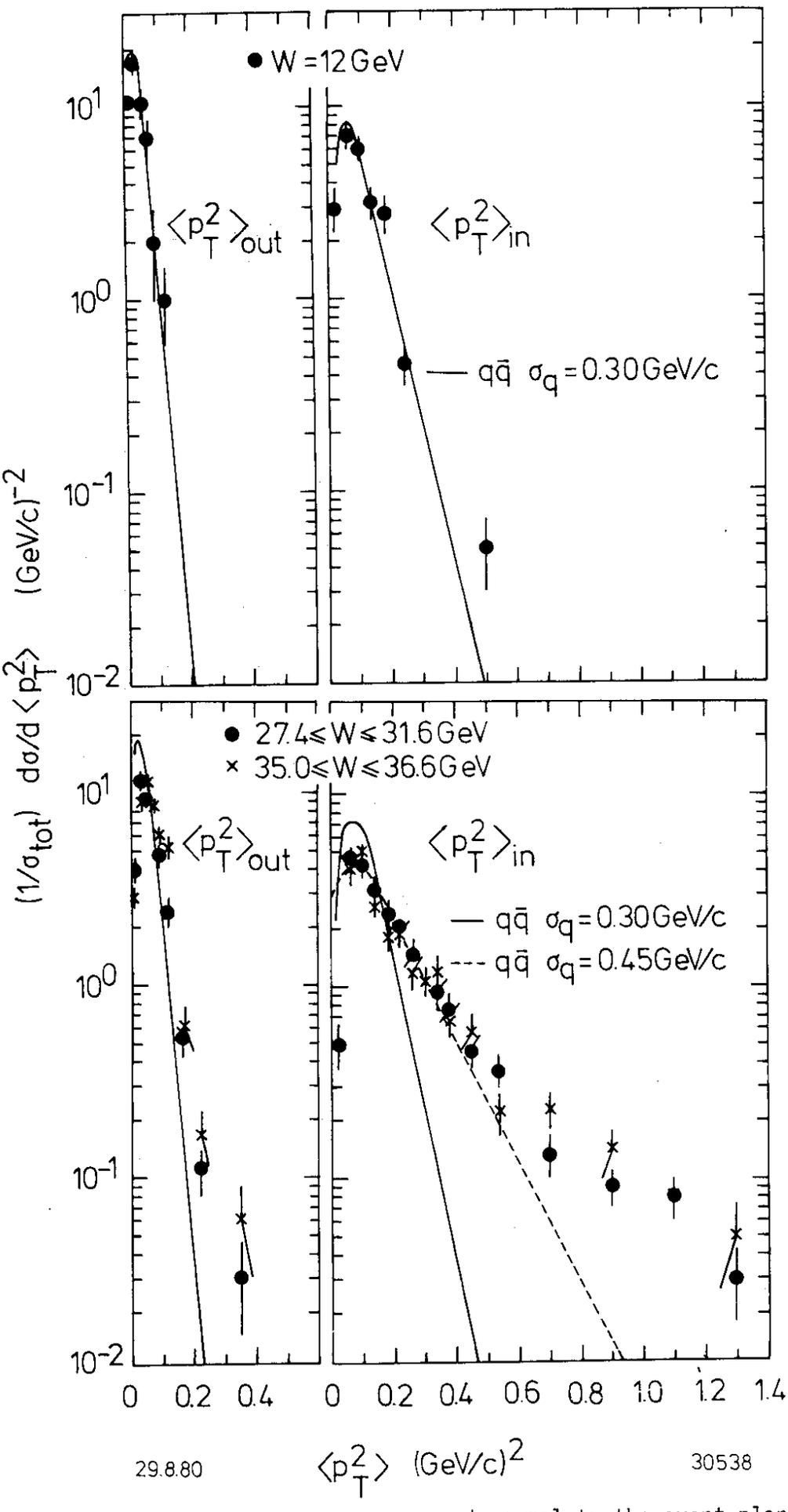

Fig. 9 The mean transverse momentum squared normal to the event plane $\langle p^2_{Tout} \rangle$ and in the plane $\langle p^2_{Tin} \rangle$ per event as measured by TASSO.

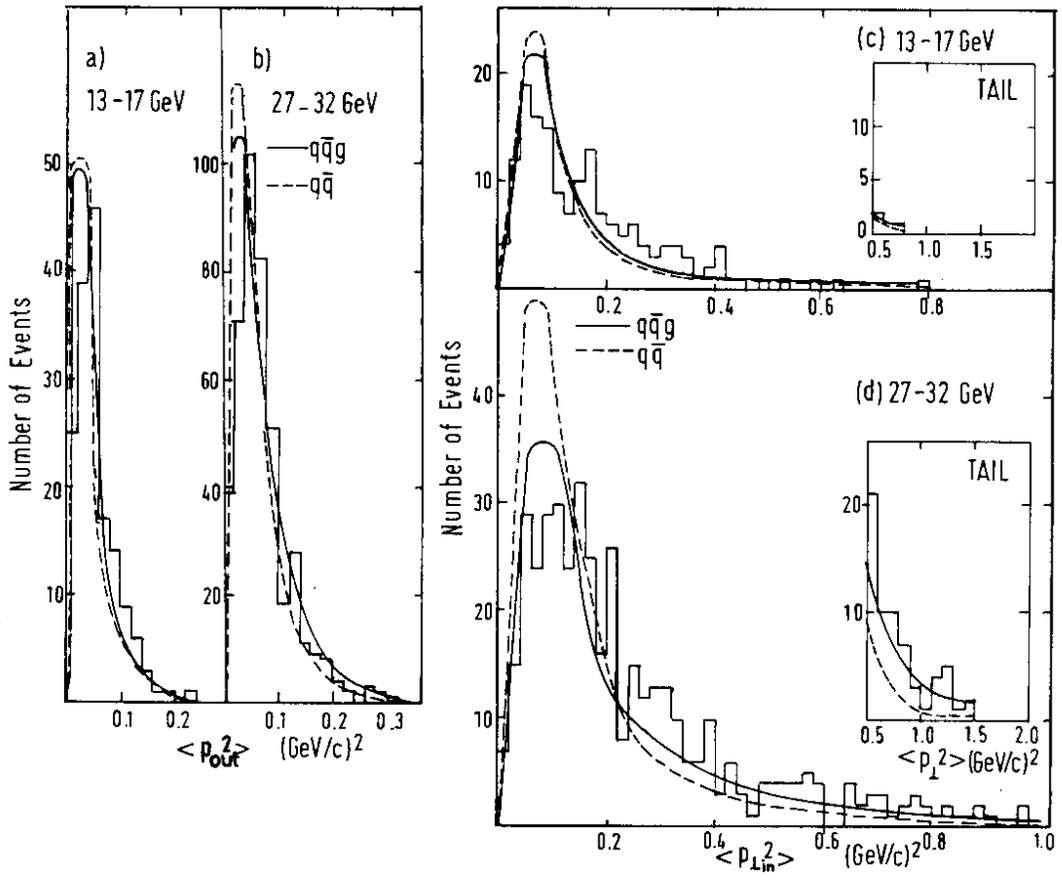

Fig. 10 Distributions of $\langle p^2_{Tout} \rangle$ and $\langle p^2_{Tin} \rangle$ as measured by PLUTO (Ref.26)

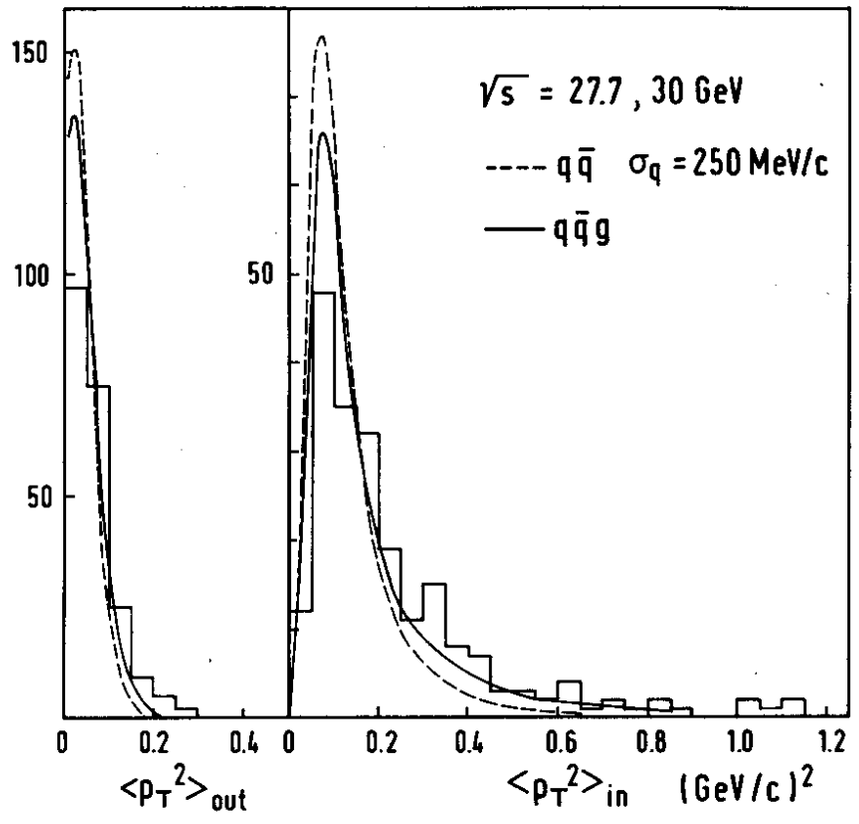

Fig. 11 Same as Fig. 10. Data measured by JADE (Ref.27).

assumption on the average p_T in that model.

The same conclusion was reached by the MARK J[28] group which studied the energy distribution ("energy flow") in the events. The coordinate system used is defined by the thrust axis ($\hat{e}_1$ = jet axis),

$$\text{Thrust} = \max. \frac{\sum_i |\vec{p}_i \; \hat{e}_1|}{\sum_i |p_i|}$$

where p_i is the energy flow detected by a counter; the major axis ($\hat{e}_2$) which is perpendicular to $\hat{e}_1$ and which is the direction along which the projected energy flow in that plane is maximized:

$$\text{Major} = \max. \frac{\sum_i |\vec{p}_i \; \hat{e}_2|}{\sum_i |p_i|} \; ;$$

the minor axis which is orthogonal to $\hat{e}_1$ and $\hat{e}_2$.

The difference Major - Minor is a measure for the planarity of an event and is called oblateness,

$$O = \text{Major} - \text{Minor}$$

The distribution of the oblateness is plotted in Fig. 12 together with the predictions of the $q\bar{q}$ and $q\bar{q}g$ models. The 17 GeV data are reproduced by both models. At the higher energies (27.4-31.6 GeV) an excess of events with large oblateness, i.e. planar events, is observed. This conclusion is reached independently of the value of σ_q used for the quark model.

The excess of planar events is readily seen at the highest PETRA energies from a plot of sphericity S versus aplanarity A (Fig.13). In this kind of plot two jet events are found near S = 0, noncollinear planar events have S > 0 but small A while for spherical events both S and A are large (Fig. 13a). For illustration Fig.13b shows the prediction of the $q\bar{q}g$ model (including u,d,s,c,b quarks) with gluon emission. The event distribution expected from a hypothetical t quark with a mass of 15 GeV which will lead to spherical events is plotted in Fig. 13c. The data shown in Fig.13d

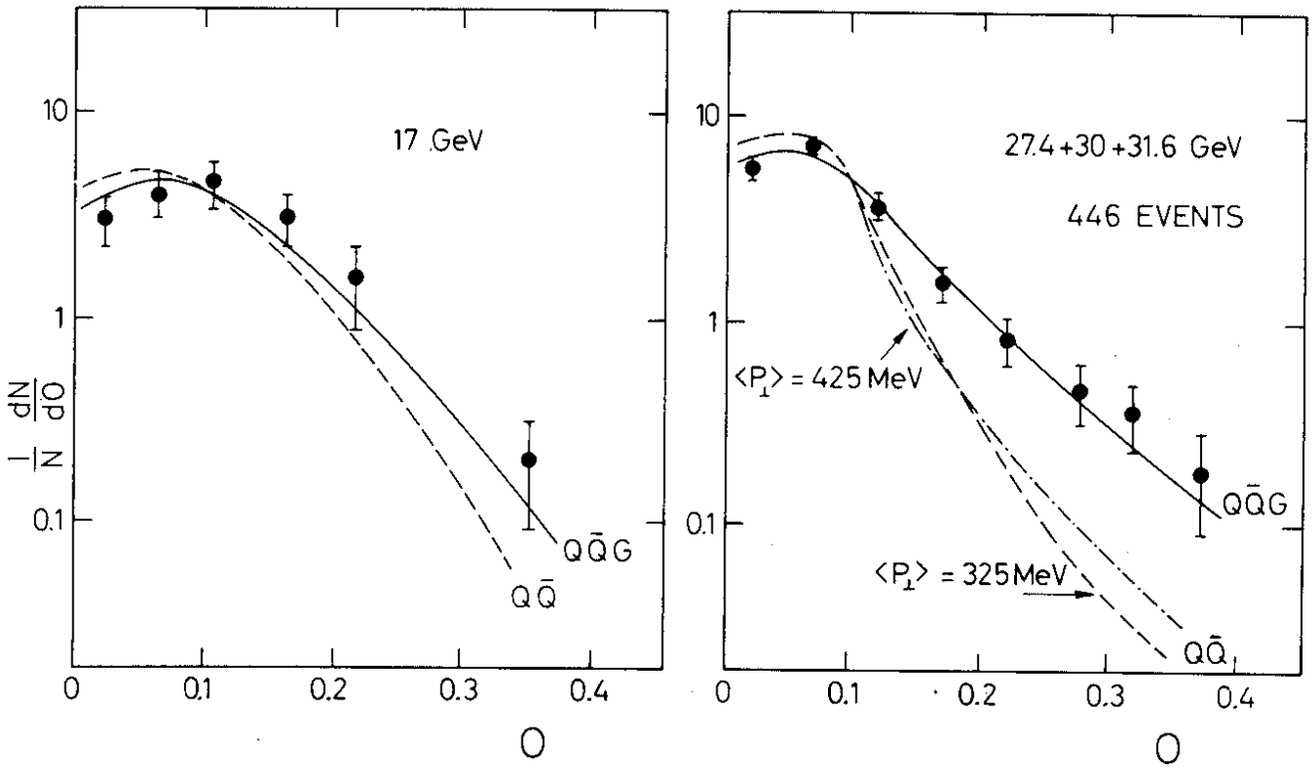

Fig. 12 The oblateness distribution, O = Major - Minor, at 17 and 27.4 - 31.6 GeV (MARK J, Ref.28)

cluster in the two-jet corner. In addition they populate a narrow band near A = 0 out to the highest sphericity values. This band of events is evidence for the presence of flat but wide = planar events.

7. Three jet structure

The data presented in the preceding paragraph demonstrated the existence of planar events. In order to check whether the particle momenta are distributed uniformly in the plane (disc like) or collimated into three jets the TASSO group adopted the procedure by Wu and Zobernig[29]. Each event is analysed as a three jet event. The particles are grouped into three classes C_1, C_2 and C_3 and for each class the sphericity is determined:

$$S_n = 3/2 \sum_{j \in C_n} \frac{q_{T_j}^2}{p_j^2}$$

The q_{T_j} are transverse momentum components in the event plane (defined by $\hat{n}_2$, $\hat{n}_3$) relative to the jet axis $\hat{n}_n$ for the group C_n which is chosen such as to minimize S_n. By considering all possible combinations one finds that grouping for which

$$S_1 + S_2 + S_3 = \text{minimum}.$$

This procedure was applied to planar noncollinear events selected by requiring $S > 0.25$, $A < 0.08$; out of a total of 777 events 77 satisfied these conditions. Fig. 14 shows the distribution of the squared transverse momenta p_T^2 of the charged hadrons for the 3 x 77 observed jets, where the p_T of each hadron is calculated with respect to the associated jet axis. It is compared with the corresponding distribution for events at 12 GeV analysed as <u>two-jets</u> and, therefore, without cuts in S or A. The p_T^2 behaviour is found to be the same in both cases, i.e., the particles from planar events at high energies are as collimated around three axis as particles from lower energy events around a single jet axis. The JADE group used the following procedure to demonstrate the existence of three-jet events. (See Fig. 15) For planar events from $W \simeq 30$ GeV selected by the condition $Q_2 - Q_1 > 0.1$ the thrust

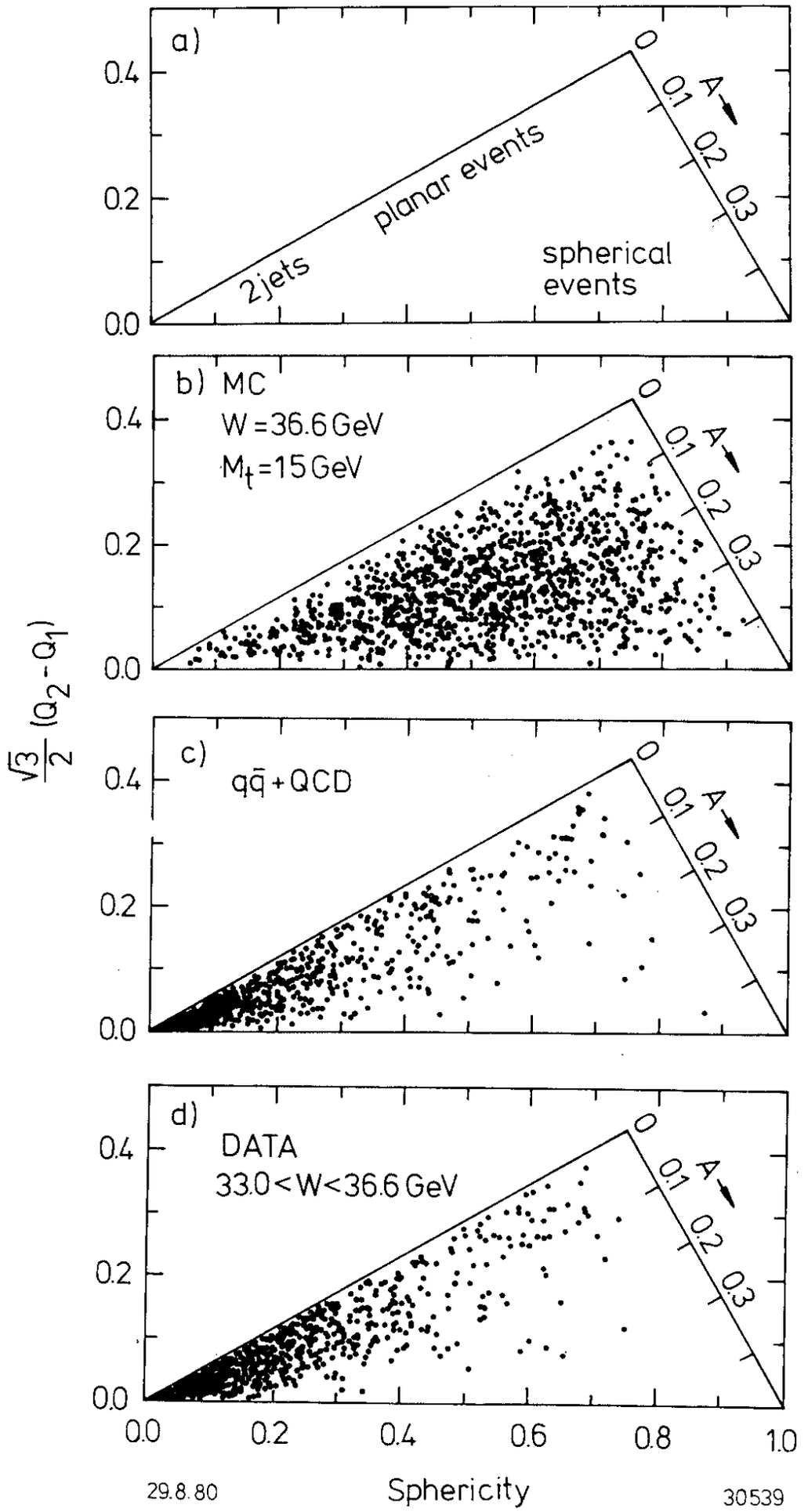

Fig. 13 Distribution of events as a function sphericity and aplanarity (TASSO).

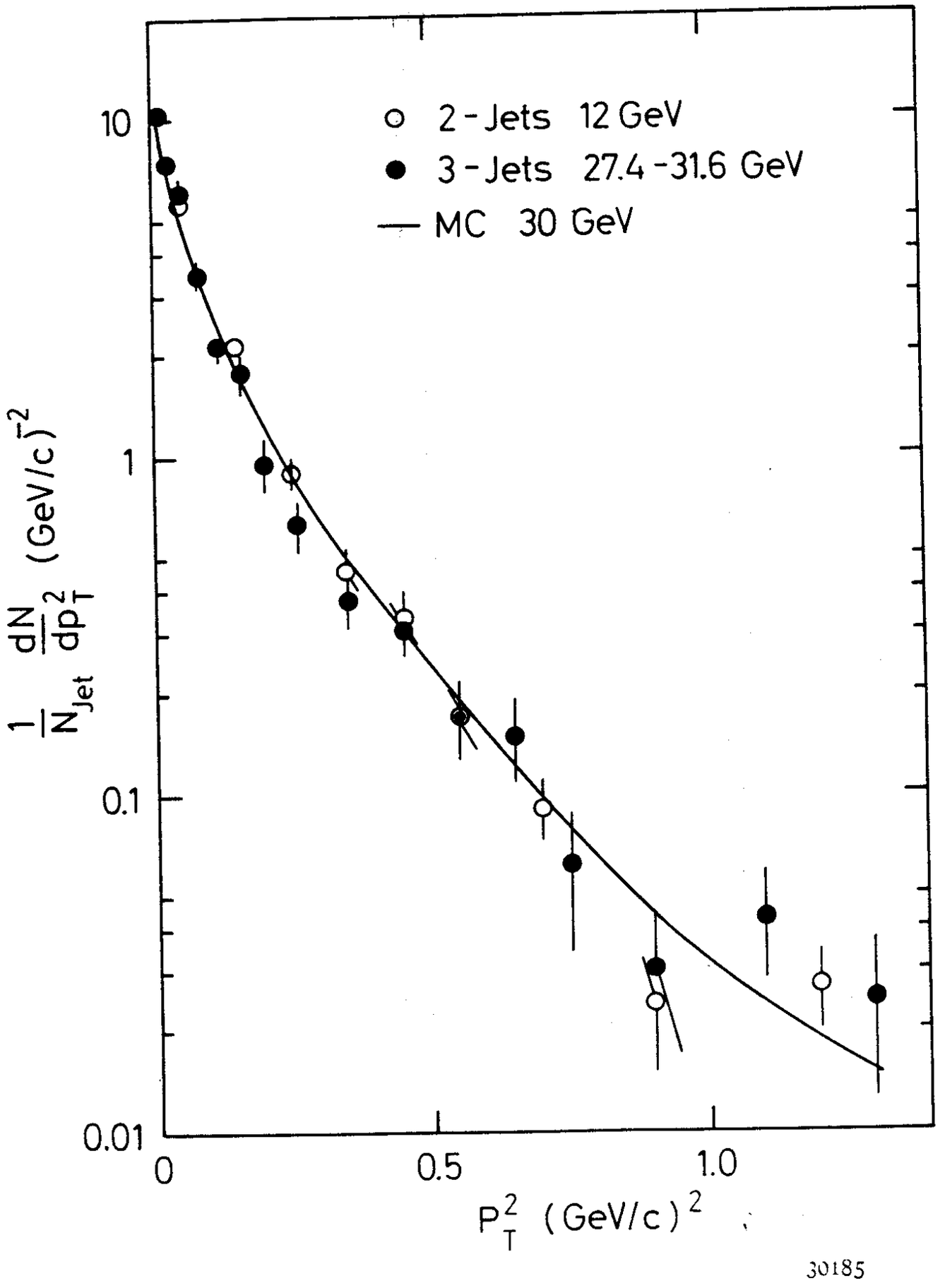

Fig. 14 Distribution of the square of the transverse momentum relative to the jet axis at 12 GeV for all events analysed as two-jet events ϕ. Distribution of the square of the transverse momentum relative to the jet axis at 27.4 - 31.6 GeV for three-jet events ϕ (TASSO).

axis was determined. For the forward and backward (with respect to the thrust axis) going particles the sum of the transverse momenta, Σp_{Ti}, was computed separately; the jet with the smaller Σp_T was called the slim jet and the other one the broad jet. The particles in the broad jet were Lorentz transformed into the rest system of the broad jet. In this system the thrust T_B of the broad jet was determined. The distribution of T_B is shown in Fig.16 together with the thrust distribution of low energy events (W = 12 GeV) treated as two-jets. The two distributions are in good agreement which leads to the same conclusion drawn before from the similarity of the p_T^2 distributions of two- and three-jet events.

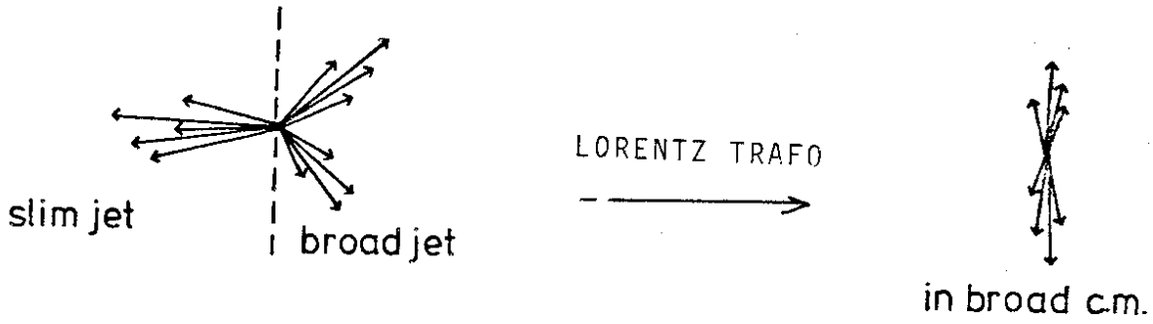

Fig. 15 Illustration of the procedure used by JADE

Fig. 17 shows a few typical three jet events.

8. Determination of α_s

The value of the quark gluon coupling strength, α_s, is directly related to the number of three jet events (see eq.(1)). In theory the determination of α_s is straightforward: after choosing a minimum angle between any pair of partons ($q,\bar{q}$ or g) the QCD cross section, eq. (5), can be integrated and compared to the corresponding observed three-jet cross section. In practise the analysis has to take into account the overlap between jets due to the hadronization, the omission of neutrals in the jet determina-

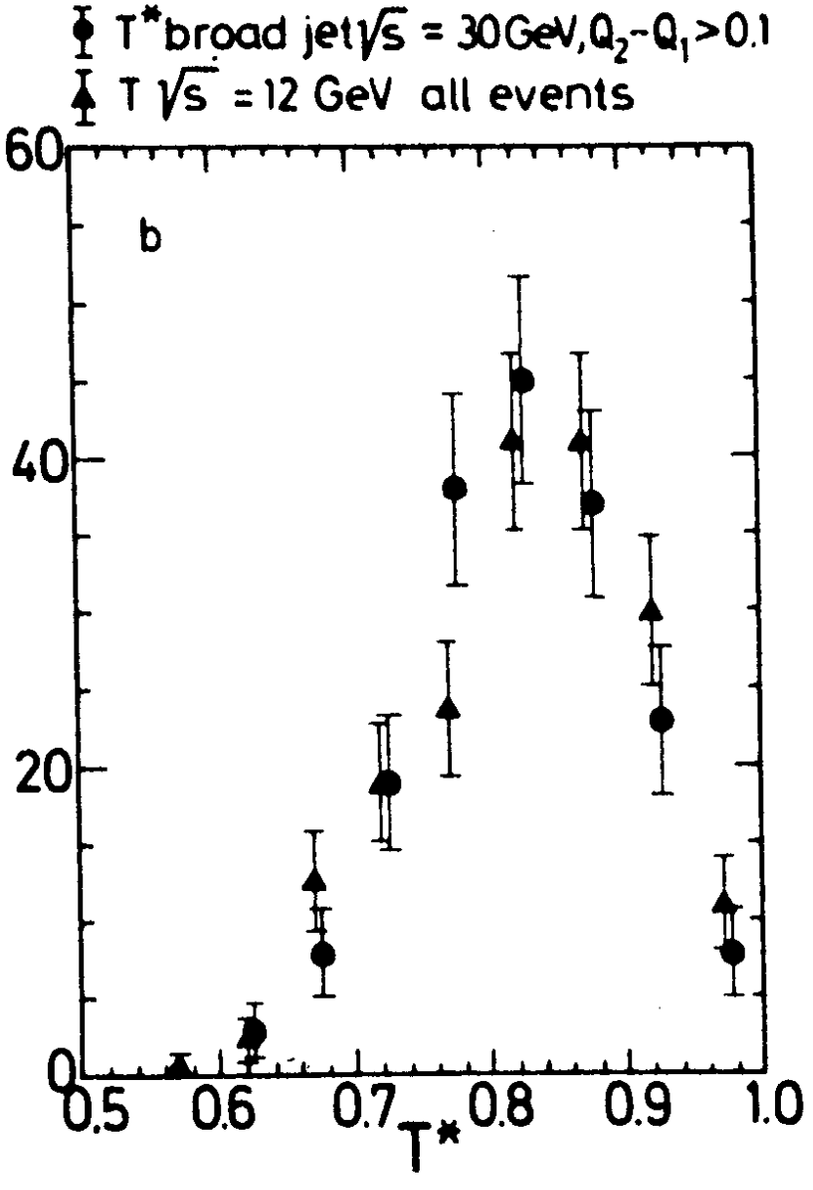

Fig. 16 Distribution of thrust for the broad jet of planar events (at 30 GeV) compared with the two-jet thrust distribution at 12 GeV (JADE)

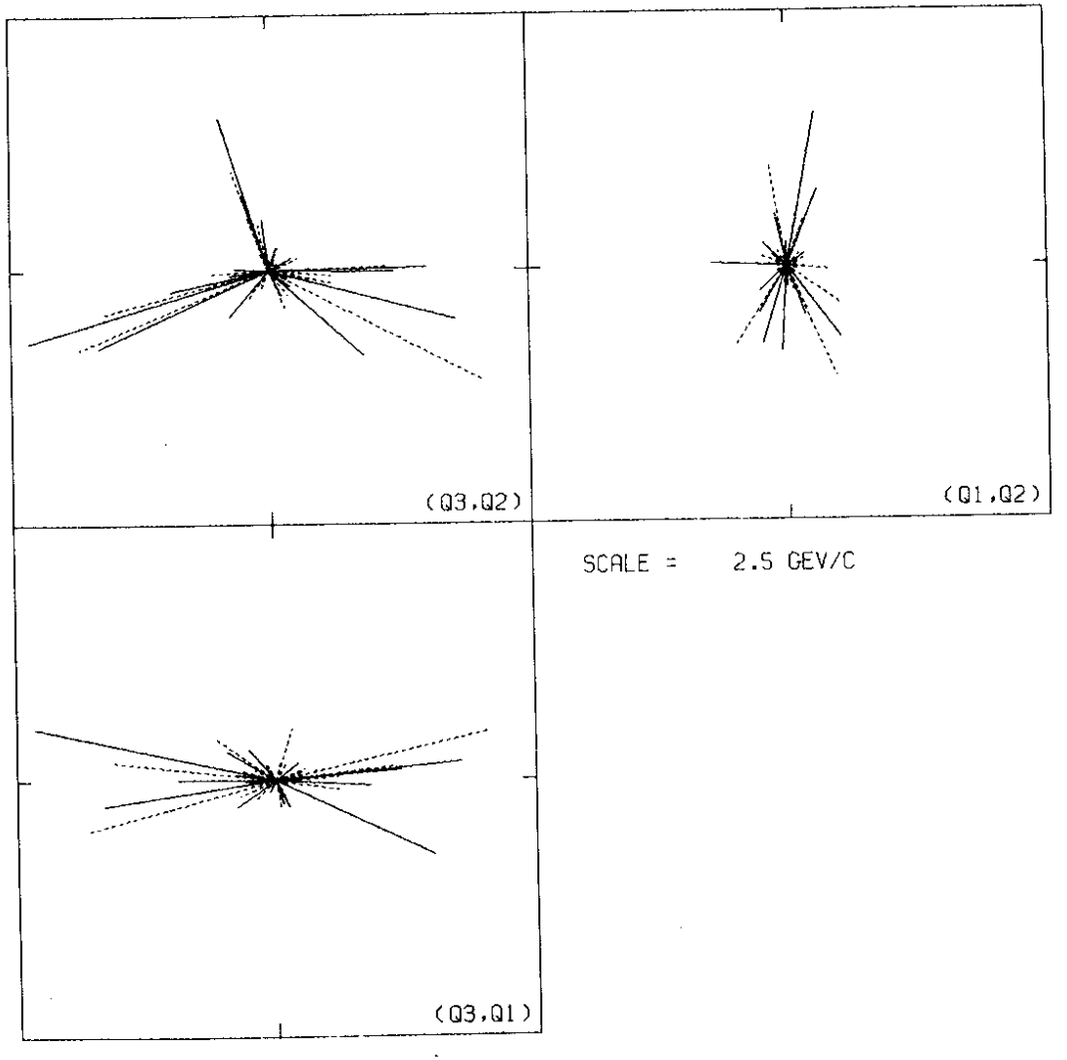

Fig. 17a The three projections of a three-jet event. The solid lines indicate charged particles, the dashed photons (JADE).

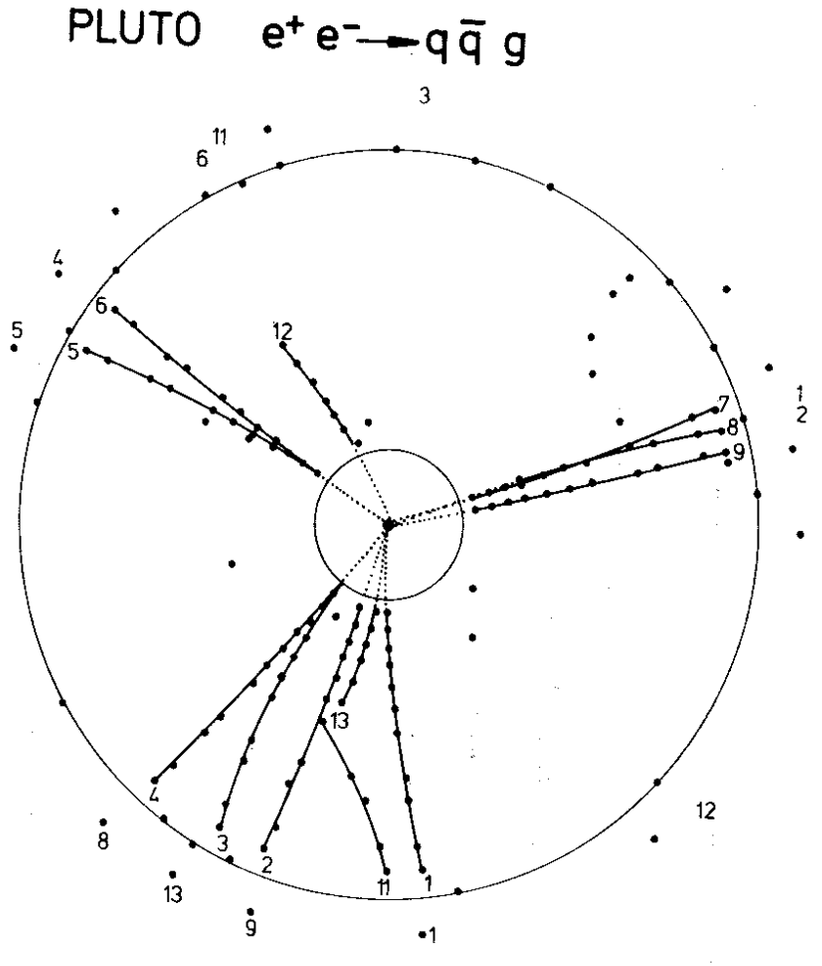

Fig. 17b A three-jet candidate from PLUTO.

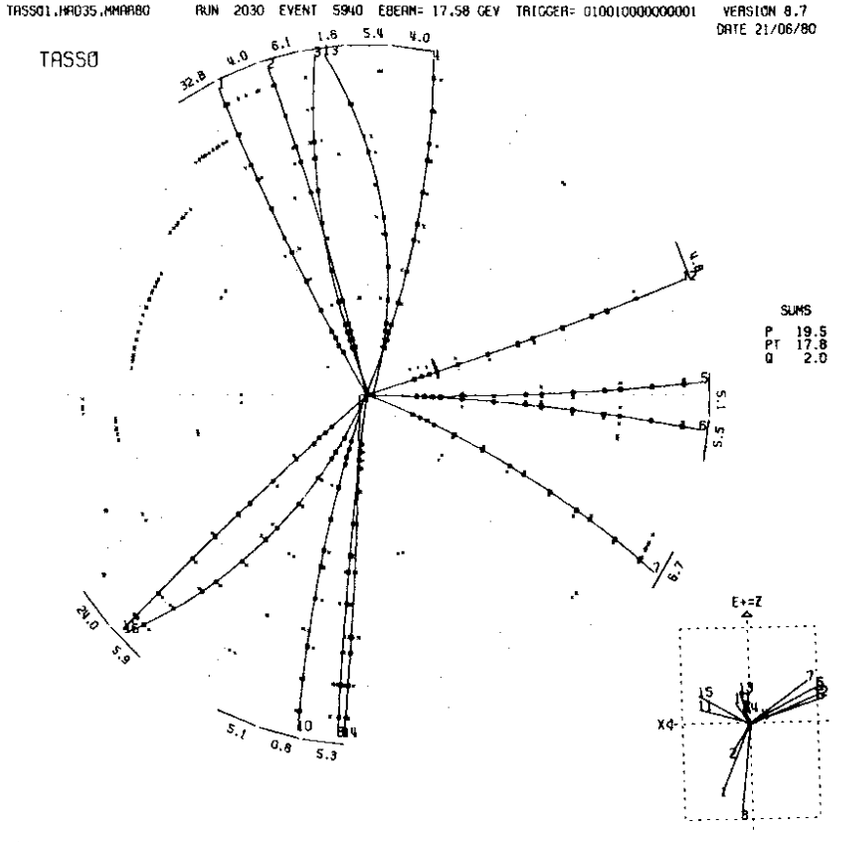

Fig. 17c A three-jet candidate from TASSO.

tion (at least in some of the experiments) plus the effect of the acceptance, the multijet contribution from semileptonic decays of the b quarks, the corrections from higher order processes in α_s. To do this, elaborate Monte Carlo codes have been employed which describe the fragmentation of the quarks and gluons into hadrons[30-32] and simulate the effects of the detector. The fragmentation parameters were fine tuned by comparison with the data. Two Monte Carlo programs have played a major role in the results obtained so far, that of Hoyer et al.[30] and an extension by Ali et al.[31]. The framework of Field and Feynman[33] is used to describe the fragmentation of quarks into hadrons. The fragmentation process involves three parameters:

(i) a_F. The primordial fragmentation function $f^h(z)$ of a quark into a hadron h,

$$q \rightarrow q' + h$$

is taken to be

$$f^h(z) = 1-a_F+3a_F\,(1-z)^2, \qquad z = \frac{(p_{||} + E)_h}{(p_{||} + E)_q} \tag{14}$$

a_F is taken to be the same for u,d and s quarks; for c and b: $a_F = 0$

(ii) σ_q. The distribution of the transverse momentum k_T of the quarks in the jet cascade is assumed to be $\sim\exp(-k_T^2/2\sigma_q^2)$.

(iii) P/(P + V). Only pseudoscalars (π,K...) and vector mesons (ρ,K*,...) are assumed to be produced. P/V is the ratio of pseudoscalar to vector mesons produced in the primordial cascade.

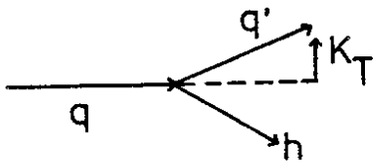

$q\bar{q}$ pairs are generated from the vacuum with the probability $u\bar{u} : d\bar{d} : s\bar{s} = 2 : 2 : 1$. Field and Feynman obtained a fair representation of hadron data with $a_F = 0.77$, $\sigma_q = 0.3$ GeV/c and $P/(P + V) = 0.5$.

In the Hoyer et al. program the gluon imparts its whole momentum to one of the two quarks (from $g \to q\bar{q}$). Therefore gluon and quark jets are the same. Ali et al. take the fragmentation function for gluons into $q,\bar{q}$, $g \to q\bar{q}$ to be[34]

$$f(z) = z^2 + (1 - z)^2, \qquad z = E_g/E_q \quad . \tag{15}$$

The quarks then turn into hadron jets according to the receipe given before.

Hoyer et al. consider only first order terms in α_s (diagrams a,b in Fig.18);

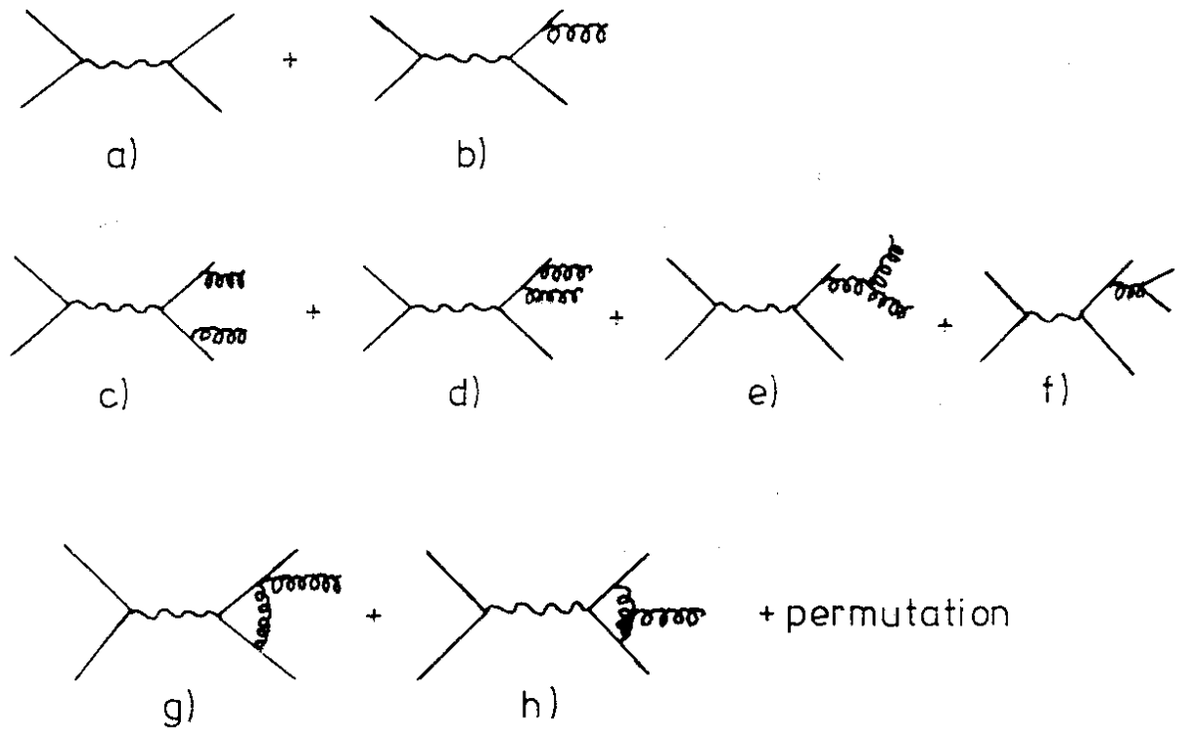

Fig.18 QCD diagram for hadron production up to second order in α_s.

Ali et al. include also all second order terms except for the diagrams of type 18g,h. In addition to the QCD diagrams QED corrections, particularly with hard photons in the initial state are important and have to be taken into account.[35]

A first attempt to determine α_s at PETRA energies was made by the MARK J group using data taken around W = 30 GeV.[36] From the oblateness distribution of the broad jet (using the Ali et al. program) a value of $\alpha_s = 0.23 \pm 0.02$ (stat.) $\pm$ 0.04 (syst.) was obtained. A recent reanalysis with the inclusion of hard photon corrections yielded a value of $\alpha_s = 0.19 \pm 0.02 \pm 0.04$ [36].

The TASSO group[37] found that α_s can be determined almost independently of the choice of parameter values describing the fragmentation by considering the events with large sphericity, $S > 0.25$. In this kinematical region three-jet events dominate and perturbative effects play a lesser role. Allowing a_F, σ_q, $P/(P + V)$ and α_s to vary, α_s was found to be 0.16 $\pm$ 0.04 independent of the values of a_F, σ_q or $P/(P + V)$.

In a second analysis the fragmentation parameters were determined using the events with small sphericity, $S < 0.25$. This region is dominated by two-jets and is insensitive to α_s. A simultaneous fit was made to

the x distribution ($x = 2p/W$) - most sensitive to a_F,
the $\langle p^2_{Tout} \rangle$ distribution - most sensitive to σ_q,
the charge multiplicity distribution - most sensitive to $P/(P + V)$,

yielding

$a_F = 0.57 \pm 0.20$, $\sigma_q = 0.32 \pm 0.04$ GeV/c, $P/(P+V) = 0.56 \pm 0.15$

With these fragmentation parameters and turning again to the events with $S > 0.25$ a more precise value for α_s was obtained which is listed in Table 1.
The JADE group followed essentially the same procedure. Their preliminary value is[38] given in Table 1. A different method was developed by the PLUTO group[39]. The events were classified as 2-, 3-, 4-jet events according to the number of particle clusters observed. The value of α_s was determined by comparing the observed and Monte Carlo predicted number of three-jet events. The result is also given in Table 1.

Table 1. Determination of α_s around W = 30 GeV.
First error is statistical, second systematic.

JADE[38]	$0.18 \pm 0.03 \pm 0.03^*$
MARK J[36]	$0.19 \pm 0.02 \pm 0.04^*$
PLUTO[39]	$0.16 \pm 0.03 \pm 0.03^*$
TASSO[37]	$0.17 \pm 0.02 \pm 0.03$

* preliminary value.

All four experiments are seen to agree on the value of α_s.

Several cautionary remarks are in order.

- Although the value of α_s was found independently of the fragmentation parameters the analyses were based on a particular way of describing the hadronization process, namely the Field-Feynman model.
- The inclusion of the second order corrections seems to have a small effect on α_s. This may be seen from the TASSO results:

$\alpha_s = 0.19 \pm 0.02$ with Hoyer et al., first order in α_s
$= 0.17 \pm 0.02$ with Ali et al., including second order terms.

However the $O(\alpha_s^2)$ calculation does not include diagrams 18 g,h, the effect of which is unknown.

Next we estimate the QCD parameter Λ using the relation

$$\alpha_s(Q^2) = \frac{12\pi}{(33 - 2N_f)\ln Q^2/\Lambda^2}$$

where N_f, the number of flavours, is taken to be $N_f = 5$.

It is theoretically an open question at which Q^2 value α_s is measured by the experiments discussed above. One possibility is to take Q^2 equal to the mass squared of the virtual photon, $Q^2 = S = W^2$, or $Q^2 \approx 900\ \text{GeV}^2$. Another choice is the mass squared P^2 of the quark that emitted the hard gluon.

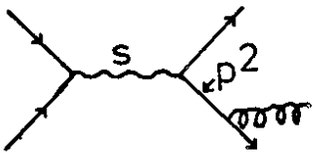

Fig. 19 shows the P^2 for the TASSO events with S > 0.25 used to determine α_s. The average P^2 is 140 GeV^2. Hence we find for

$$\alpha_s = 0.17 \pm 0.02 \pm 0.03$$

$$Q^2 = S: \quad \Lambda = 240 \begin{cases} \nearrow 410 \to 730 \\ \searrow 130 \to 30 \end{cases} \text{ MeV}$$

$$Q^2 = P^2: \quad \Lambda = 95 \begin{cases} \nearrow 160 \to 290 \\ \searrow 50 \to 12 \end{cases} \text{ MeV}$$

This range of Λ values may be confronted with the result from deep inelastic μp and γN scattering. The high Q^2 data indicate $\Lambda \approx 100$ to 500 MeV.

We close this section with a few figures in order to demonstrate how well the data are reproduced using the fragmentation parameters and the value α_s given above. Fig.20 shows the measured sphericity, aplanarity and x distributions at W=12 and 30 GeV together with curves calculated from the model. Note that only the W = 30 GeV data were usedin the fit;at W = 12 GeV the curves are genuine predictions. Fig. 21 shows the fit to the $\langle p^2_{Tout} \rangle$ distribution.

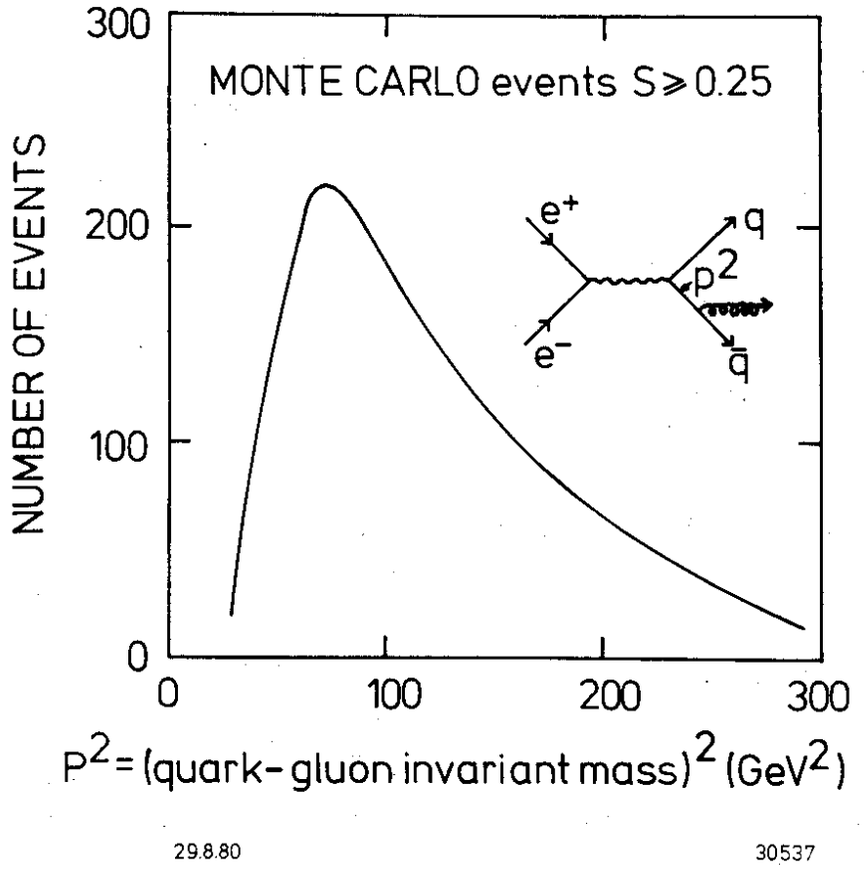

Fig. 19 Distribution of the square of the quark-gluon mass as computed with the MonteCarlo of Ali et al for events with large sphericity.

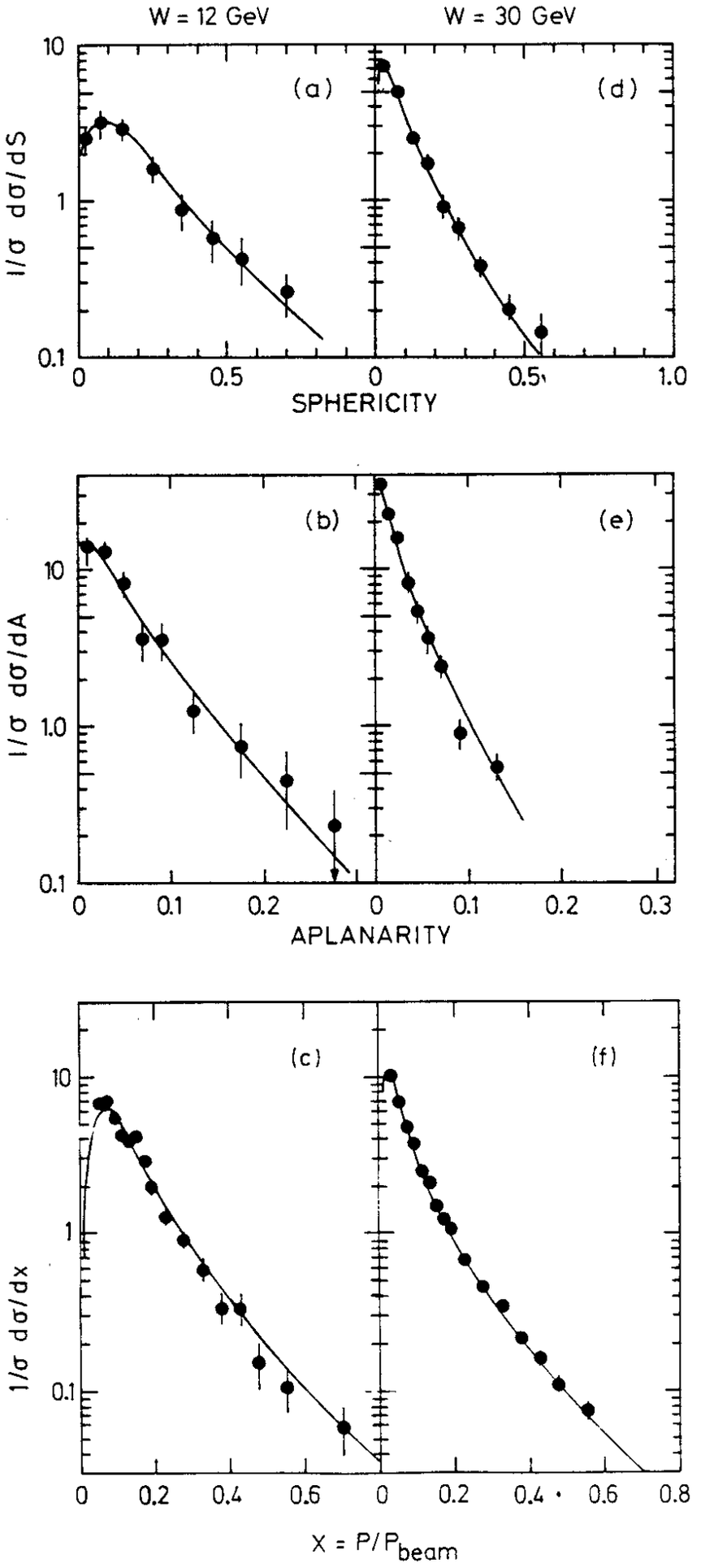

Fig. 20 Comparison fo the data for sphericity, aplanarity and the single particle inclusive x distribution for charged particles at 12 and 30 GeV with the QCD model (curves). From TASSO, Ref. 37.

9. Is there a difference between quark and gluon fragmentation?

There are several qualitative arguments which say that quarks and gluons fragment differently:

- A gluon before hadronization has to turn into a $q\bar{q}$ pair. Hence there are at least two quarks ($q=\bar{q}$) per gluon which then fragment into hadrons.
- The ggg coupling is 9/4 times stronger than that for qqg (9/4 α_s versus α_s). Therefore gluon emission is more frequent for gluons than for quarks.

Both arguments favour a higher hadron multiplicity for gluon jets.

Andersson, Gustafson and collaborators[40] suggested to study the yields of low energy particles emitted at large angles to the jet axes.

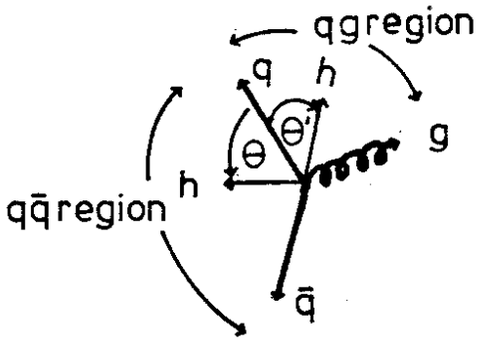

The JADE group[41] performed the analysis using charged and neutral particles. Like before, planar events with $Q_2 - Q_1 > 0.07$ were grouped into the slim jet (q) and the two subjets which make up the broad jet. The subjet with the smaller angle relative to the slim jet was called the gluon jet (g), the other one the quark jet ($\bar{q}$). Monte Carlo studies indicate that in this way the gluon is correctly assigned for ~70 % of the events. The particle yield was then measured as a function of the angle Θ between the particle and the slim jet. In Fig. 22 the particle yield is shown as a function of Θ/Θ_{max} for the $q\bar{q}$ and the qg regions. One observes a significant difference (4 s.d.) near $\Theta/\Theta_{max} \approx 0.5$: the particle density is two times larger in the qg compared to the $q\bar{q}$ region. Fig. 22 was determined with charged and neutral particles. Charged particles alone reportedly give the same result. The Hoyer et al. MC does not predict a difference if the quark and gluon fragmentations are treated identically. The Lund MC[32] agrees with the data.

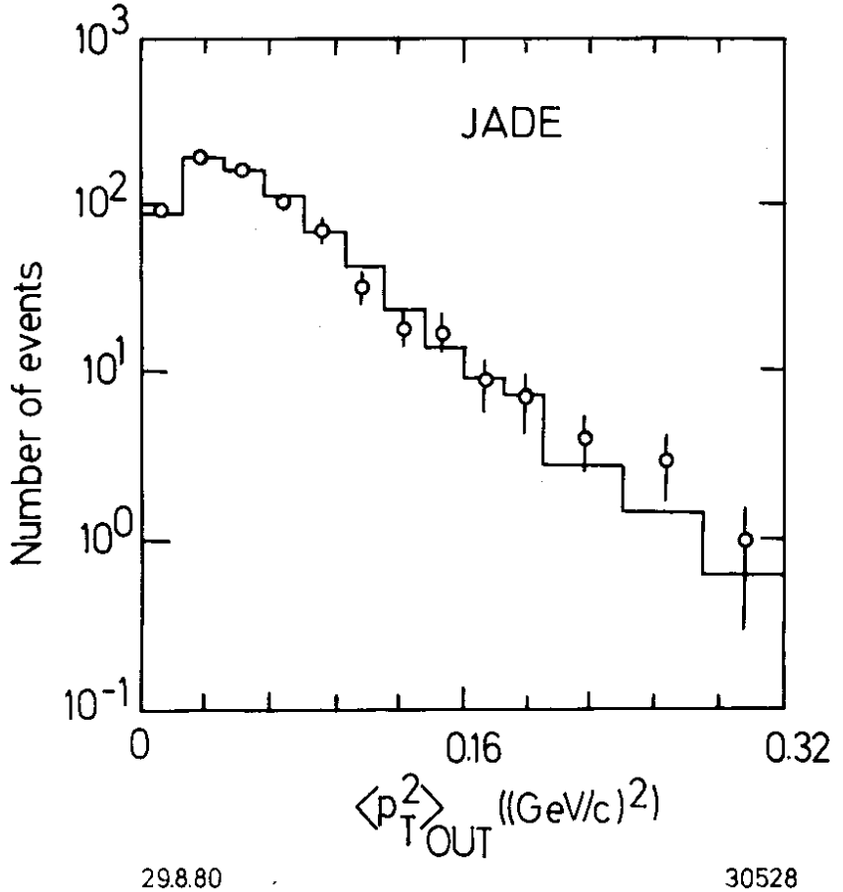

Fig. 21 Comparison of the $\langle p_{T\,out}^2 \rangle$ distribution at 30 GeV with the QCD model (histogram). From JADE.

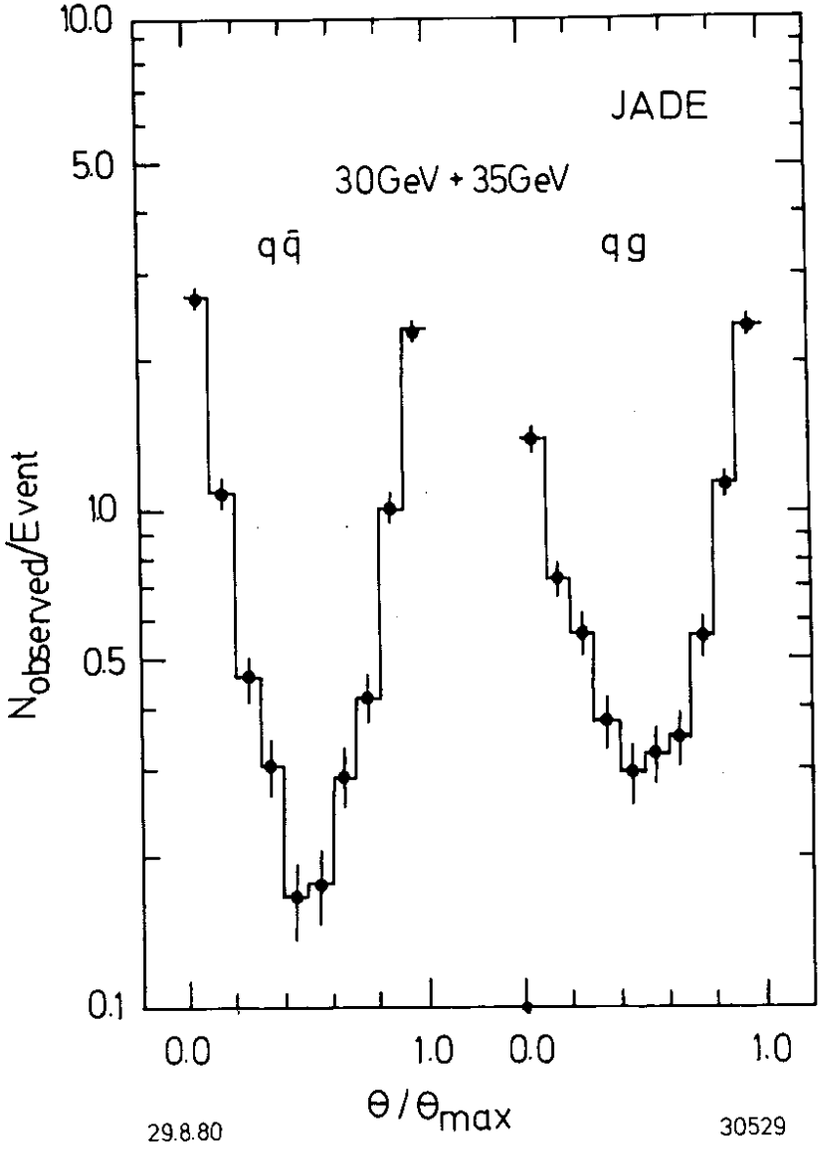

Fig. 22 Angular distribution Θ/Θ_{max} of particles between the jet axes (see text). From JADE

This may be the first experimental indication that quarks and gluons fragment differently.

10. Soft gluon emission

The previous section primarily dealt with effects due to the emission of a single hard gluon. This section considers the emission of soft gluons. For soft gluons α_s is no longer small but of order unity. Many (infinitely many) diagrams become important and should be summed. No rigorous theory does exist yet but a first step towards understanding these processes theoretically as well as studying them experimentally was made.

Consider again gluon bremsstrahlung in $e^+e^- \to q\bar{q}g$.

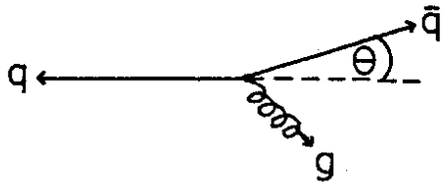

The cross section diverges as the angle Θ between the -q and $\bar{q}$ directions goes to zero,

$$\frac{d\sigma}{d\Theta} \sim \frac{1}{\Theta}$$

This divergence is cancelled by multigluon emission (see sketch).

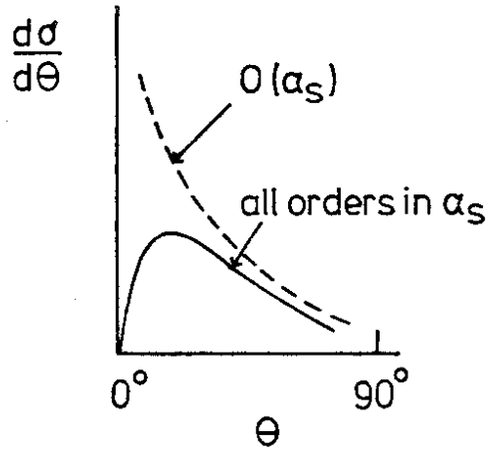

The cross section approaches zero as $\Theta \to 0$: quark and antiquark are never emitted exactly back-to-back.

Dokshitzer, D'Yakanov and Troyan[42] proposed to relate the parton angular distribution to the two particle differential cross section:

$$\frac{1}{\sigma}\frac{d\Sigma}{d\Theta} = \sum_{a,b} \int dx_a \, dx_b \, x_a \, x_b \, \frac{1}{\sigma} \frac{d\sigma}{dx_a dx_b d\Theta} \qquad (16)$$

where a,b are any two particles emitted in the event with fractional momenta x_a, x_b, $x = P/E_{beam}$ and angle $(\pi-\Theta)$ between them, and summation is performed over all two particle combinations.

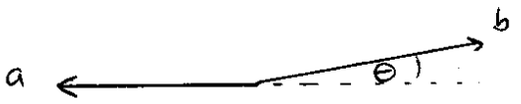

Through the factor $x_a x_b$ the higher momentum particles which supposedly know more about the primary quark directions are weighed more heavily.

The PLUTO group determined the two particle differential cross section $\frac{1}{\sigma}\frac{d\Sigma}{d\Theta}$ at energies between 9.4 and 31.6 GeV.[43] Fig. 23 shows the result at 31.6 GeV for the small angle region. The cross section tends to go to zero as $\Theta \to 0$; it goes through a maximum and falls off towards large angles.

The curves shown in Fig. 23 were computed by Ref.44 at the quark level, i.e. hadronization was not considered. The curve labelled $O(\alpha_s)$ illustrates what was said before: the first order term diverges as $\Theta \to 0$. The curves labelled $\Lambda = 0.2$ and $\Lambda = 0.8$ were computed in the leading log approximations to all orders in α_s. They show explicitly the large cancellation near $\Theta = 0$ forcing the cross section to go to zero as $\Theta \to 0$. However, the hadronization process, which was not included in the calculation and which affects particularly the small Θ region, may change the whole picture.

Refs. 45 and 46 made an attempt to include hadronization effects.

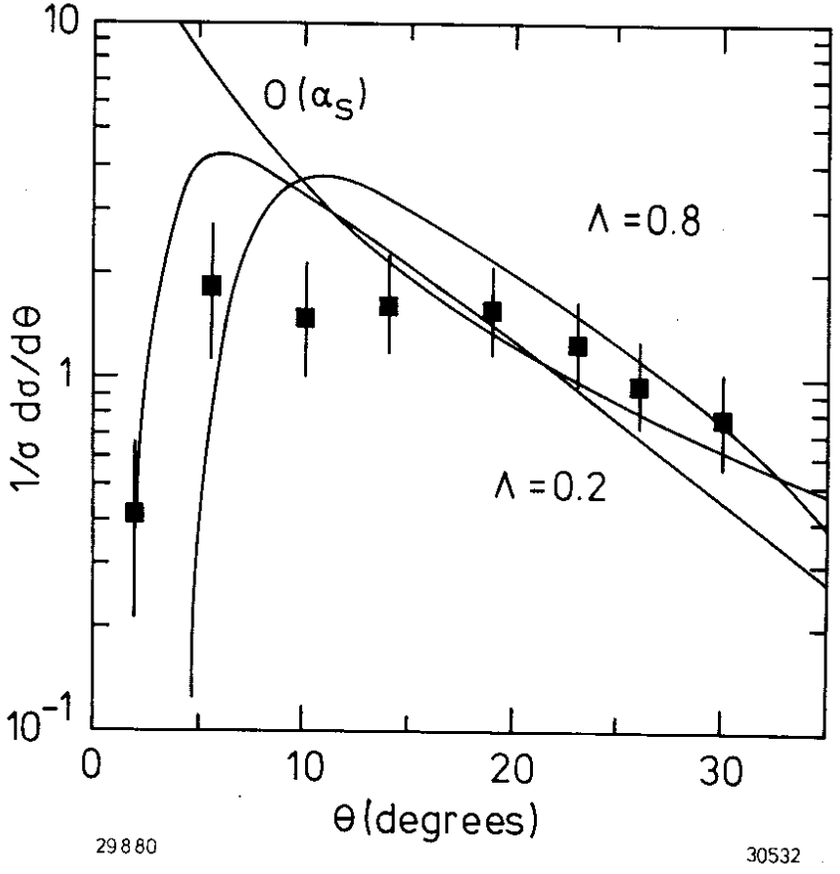

Fig. 23 The two-particle cross section (eq.16) as measured at 30 GeV by PLUTO (Ref. 43). The curves show the prediction of single gluon bremsstrahlung and of the leading log approximation without hadronization[44].

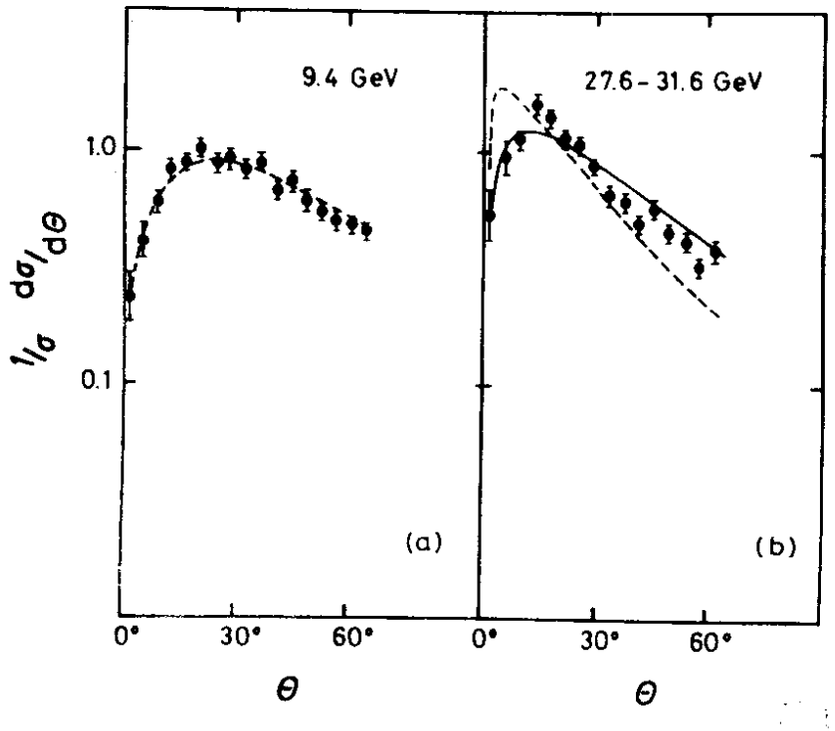

Fig. 24 The same quantity as in Fig. 23 at 9.4 and 30 GeV. The dashed curve in (b) was calculated in the leading log approx., the solid curve includes hadronization[46].

In Ref.46 the PLUTO data at 9.4 GeV where hard gluon effects are small were used to fix the parameters of hadronization. Assuming that after hard gluon emission the partons transform independently into hadrons the two particle differential cross section was predicted at 30 GeV using the leading log approximation and a QCD evolution technique.

Fig. 24 shows the input data at 9.4 GeV and the 30 GeV data together with their prediction (solid curve) which describes the data well. The dashed curve was computed without hadronization. The difference between the dashed and the solid curves demonstrates the importance of the hadronization process.

Two particle correlations at large angles were studied theoretically in papers cited in Ref. 47.

11. Gross features of the final states

As we saw above the final states in high energy e^+e^- annihilation are a result of quark and gluon induced jet formation. Correspondingly, by analysing the final state particles one should be able to piece the jet fragments together and reconstruct the properties of the primordial parton, such as charge, flavour, etc. This section summarises briefly what is known on the final states produced at high energies.

11.1 Energy carried by neutrals

The JADE group[41,48] measured the fraction of energy carried by photons (either from π^0,η.. decay or from direct production) and by neutrals:

$$f_\gamma = \frac{\sum_i E_{\gamma_i}}{W}$$

and

$$f_{neutral} = 1 - \frac{\sum_i E_{CHi}}{W}$$

E_{CHi} energy of charged particle i.

$f_{neutral}$ includes K^0_S and Λ particles. The result is given in Table 2 for energies between 12 and 35 GeV.

Table 2. Fraction of energy carried by photons and neutrals

W(GeV)	f_γ(%)	$f_{neutral}$ (%)
12	21.3 ± 7.0	31.2 ± 4.1
30.4	26.1 ± 5.9	37.5 ± 3.7
34.9	30.7 ± 6.0	43.8 ± 4.1

Furthermore, the fraction of energy carried by neutrinos, f_ν, was found to be less than 15 % (2 s.d.) at all energies. If free quarks of unit charge à la Pati-Salam exist f_ν should be equal to 20 to 30 %.

11.2 Charged particle multiplicity

In Fig. 25a the average charged particle multiplicity* $\langle n_{CH} \rangle$ is plotted as a function of c.m. energy[49]. Above ~7 GeV the multiplicity is seen to rise (logarithmically) faster than at lower enerbies. The curves give the energy dependence for pp collisions[56] and $\bar{p}p$ annihilation[57]. They seem to bracket the e^+e^- data at high energies**.

The simplest form of scaling of charged particle production leads to $\langle n_{CH} \rangle = a + b \ln s$. This is certainly at variance with the data if the full energy range is considered. The observed rise of $\langle n_{CH} \rangle$ cannot be attributed to the onset of $b\bar{b}$ production which is found to yield an increase by ~ 0.2 units. In QCD an increase of $\langle n_{CH} \rangle$ over the scaling curve is predicted due to the additional contribution from gluon fragmentation. The exact form of the resulting

---

* $\langle n_{CH} \rangle$ includes the $\pi^\pm$ coming from $K^0_S \to \pi^+\pi^-$ decay. This contribution amounts to 0.4 units at 7.4 GeV, 0.6 at 12 GeV and 1 unit at 30 GeV. In the pp and $\bar{p}p$ data shown by the curves the K^0_S contribution is not included.

** An interesting comparison between e^+e^- and pp data has been performed in Ref. 58 where the leading protons have been subtracted and the c.m. energy was rescaled. In this analysis a close correspondence between pp and e^+e^- data is obtained.

energy dependence is not yet clear. If the result for infinitely heavy quarks is taken for guidance, one expects $\langle n_{CH} \rangle$ to grow like[59]

$$\langle n_{CH} \rangle = n_o + a \exp(b\sqrt{\ell n(s/\Lambda^2)}) .$$

Fits of this form reproduce the trend of the data[54,55]. One may therefore be tempted to attribute the rapid rise to hard gluon effects. However, Fig.25b compares the $\langle n_{CH} \rangle$ data with the $q\bar{q}$ model, $e^+e^- \to q\bar{q} \to$ hadrons using the Field-Feynman fragmentation functions but <u>without</u> hard gluon contributions. The model accounts well for the rise seen above ~5 GeV (see dashed curve)*. The inclusion of hard gluon emission raises the prediction by a negligible amount below 10 GeV; at 35 GeV it adds 0.8 units. We conclude therefore that the rapid rise of $\langle n_{CH} \rangle$ is mostly due to the growing phase space: the particle masses matter less as the energy goes up.

In Fig.26a the PLUTO group[55] has compared the e^+e^- multiplicity distributions in a KNO plot[60] with pp and $\bar{p}p$ data. Plotted is $P_{CH} \cdot \langle n_{CH} \rangle$ where P_{CH} is the probability for observing a final state with n_{CH} charged particles versus $n_{CH}/\langle n_{CH} \rangle$. The e^+e^- data obey KNO scaling between 9.4 and 30 GeV. The distribution agrees well with the $\bar{p}p$ data but disagrees with the pp data which have a larger dispersion (see also Fig.26b),

11.3 Inclusive particle spectra without particle identification

The differential cross section for producing a particle h with momentum and energy P, E and angle Θ relative to the beam axis can be expressed in terms of two structure functions $\bar{W}_1$ and $\bar{W}_2$ which are closely related to W_1 and W_2 measured in inelastic lepton hadron scattering[61]

$$\frac{d^2\sigma}{dx d\Omega} = \frac{\alpha^2}{s} \beta x \{m\bar{W}_1 + \frac{1}{4} \beta^2 x \nu \bar{W}_2 \sin^2\Theta\} \qquad (17)$$

where m is the mass of h, $\beta = P/E$, $x = E/E_{beam} = 2E/\sqrt{s}$ and ν is the energy of the virual photon as seen in the h rest system, $\nu = (E/m)\sqrt{s}$.

*At lower energies the model is presumably less reliable because of the approximations made for the fragmentation.

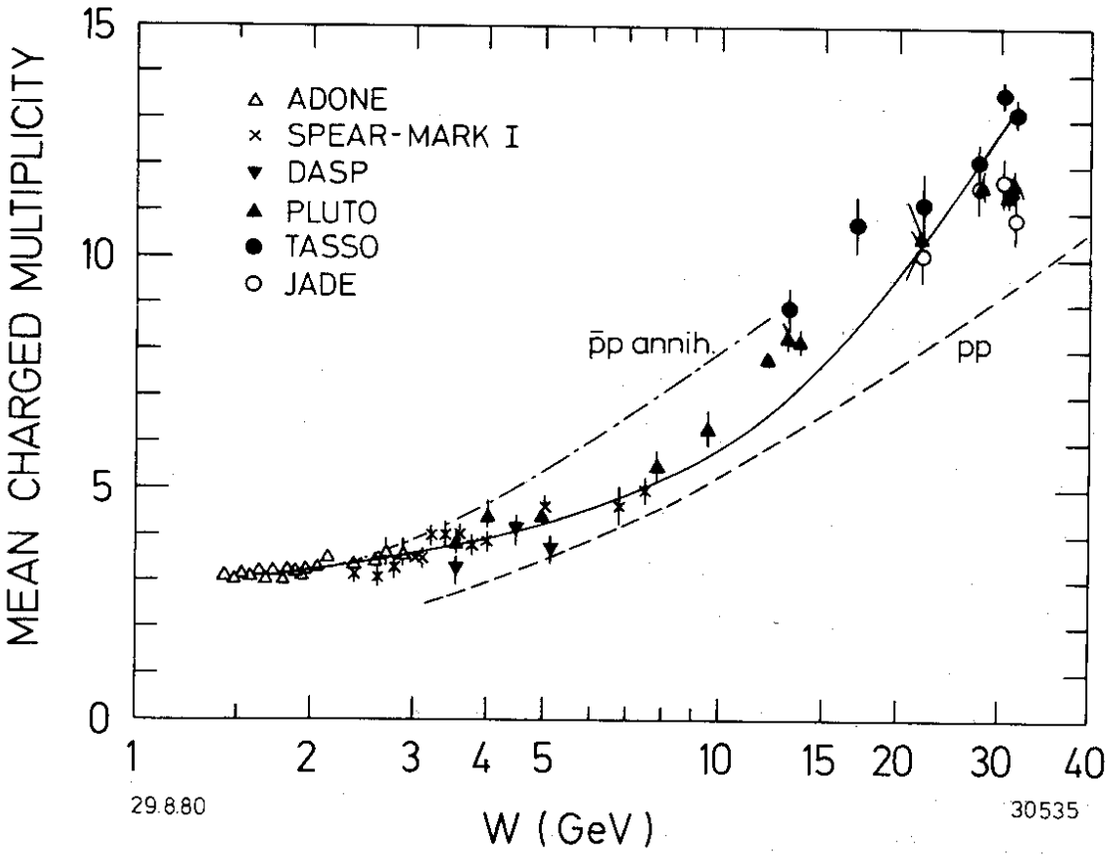

Fig. 25a Average charged particle multiplicity as a function of c.m. energy.

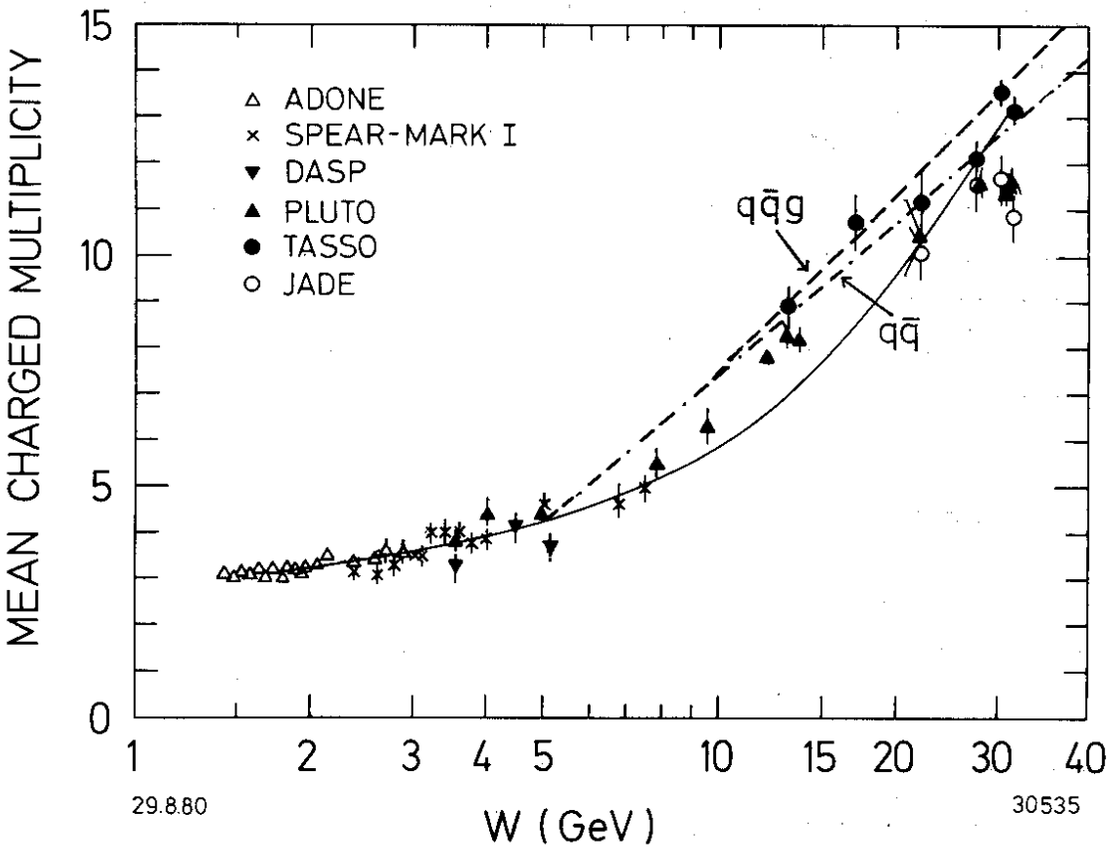

Fig. 25b Same as in Fig. 25. The dashed-dotted and dashed curves show the predictions of the $q\bar{q}$ and $q\bar{q}g$ models.

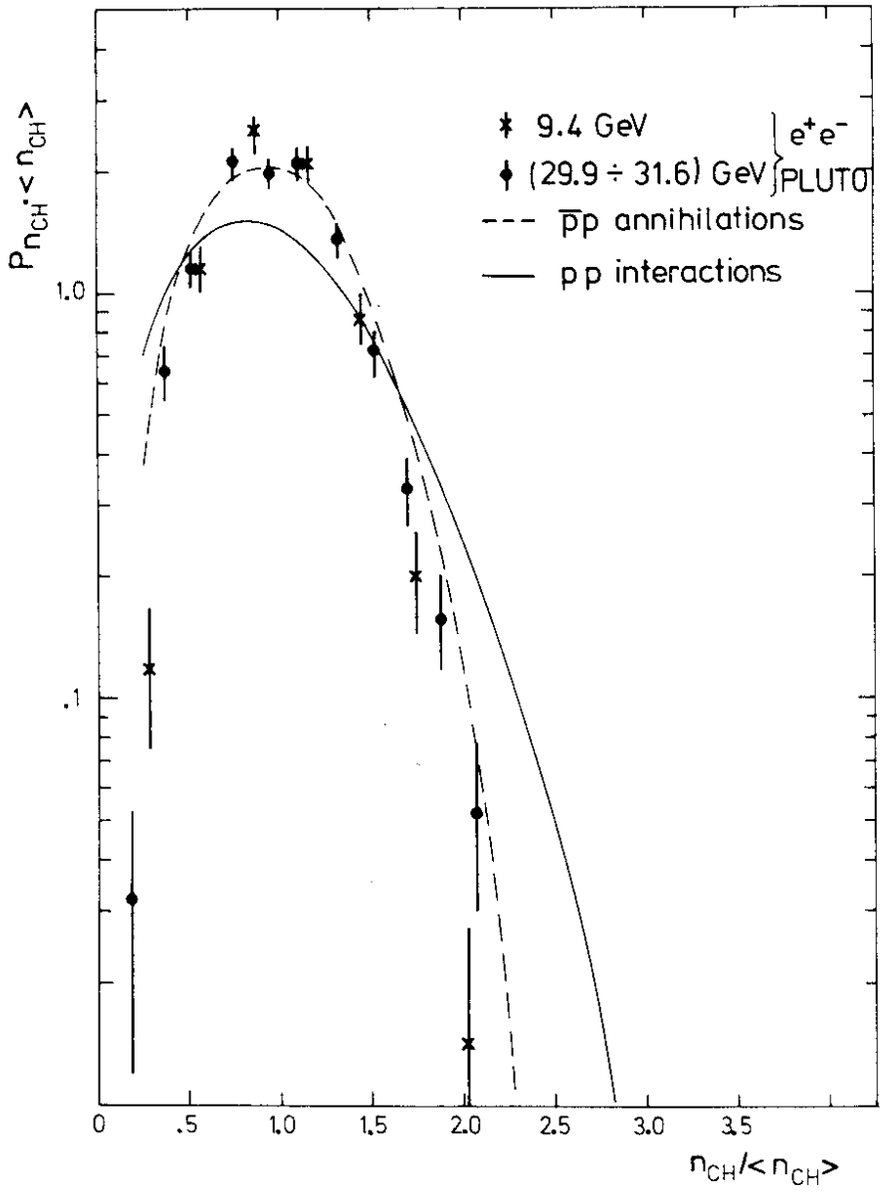

Fig. 26a KNO plot for e^+e^- data as measured by PLUTO at 9.4 and 30.7 GeV[55]. The dashed curve is a fit to $p\bar{p}$ annihilation data. The solid curve describes high energy pp data.

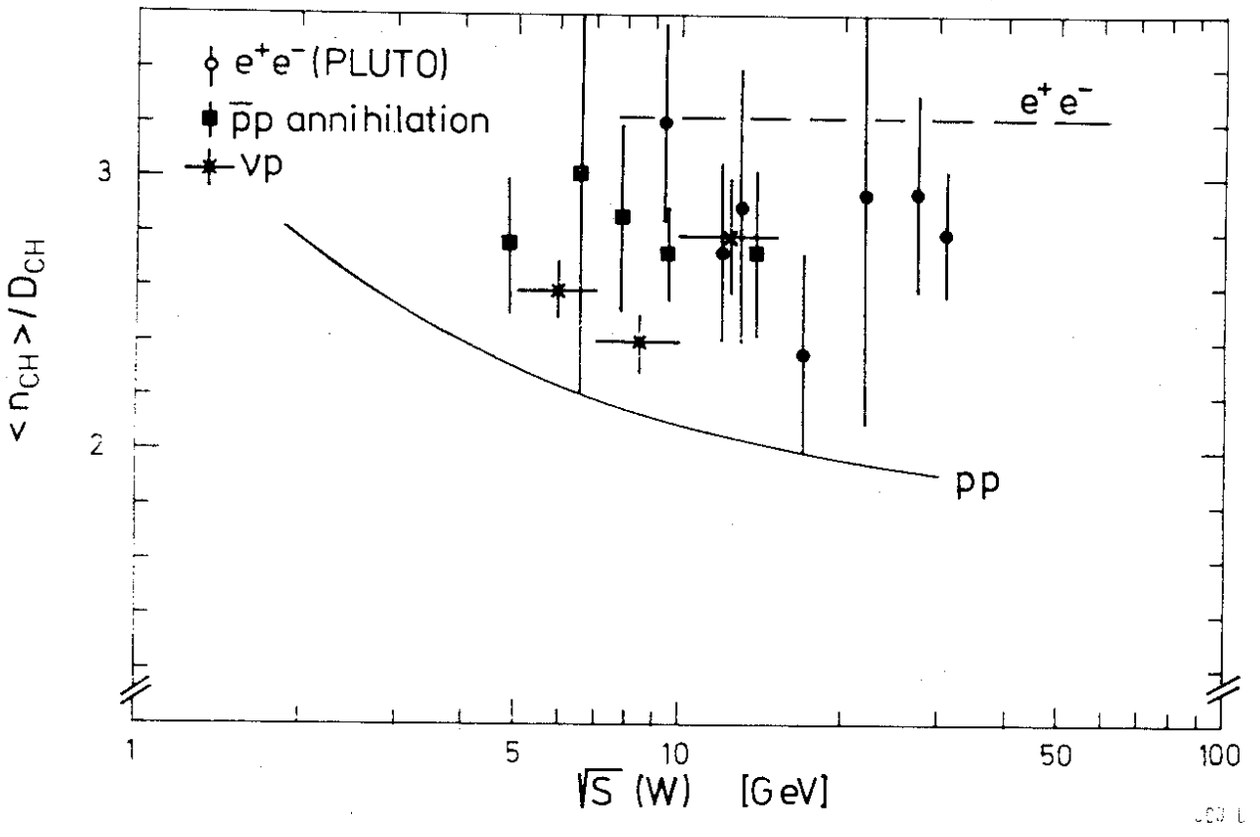

Fig. 26b Energy dependence of the ratio $\langle n_{CH}\rangle/D_{CH}$ where $\langle n_{CH}\rangle$ is the mean charge multiplicity and D_{CH} is the dispersion of the multiplicity distribution, $D_{CH} = \sqrt{\langle n_{CH}^2\rangle - \langle n_{CH}\rangle^2}$. Also shown are the data for pp interactions, $\bar{p}p$ annihilations and νp interactions. (From PLUTO[55]).

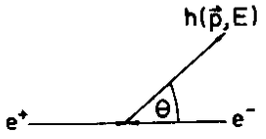

Diagram for inclusive particle production.

At particle energies large enough that particle masses can be neglected, x can be replaced by the normalized momentum $x = P/E_{beam}$ and the scaling cross section reads

$$s d\sigma/dx \approx 4\pi\alpha^2 \times \{m\bar{W}_1 + \frac{1}{6} \times \nu\bar{W}_2\} \qquad (18)$$

The structure functions in general depend on two variables, e.g. x and s. If scale invariance holds $\bar{W}_1$ and $\nu\bar{W}_2$ are functions of x alone and $sd\sigma/dx$ is energy independent.

Scaling behaviour is e.g. expected from the hypothesis of quark fragmentation: at energies large enough that particle masses can be neglected, the number of hadrons h produced by a quark q with fractional energy x, $D_q^h(x)$, is independent of s. This leads to

$$\frac{d\sigma}{dx}(e^+e^- \to q\bar{q} \to h) = \sigma_{q\bar{q}} \cdot 2D_q^h(x) = \frac{8\pi\alpha^2}{s} e_q^2 D_q^h(x) \qquad (19)$$

Fig. 27 displays the data on $sd\sigma/dx$ measured by TASSO[62,63] at energies between 12 and 36 GeV. For $x > 0.2$ they are the same within errors and agree with those measured at low energy by DASP (Ref. 64, 5 GeV) and SLAC-LBL (Ref. 65, 7.4 GeV) to within 30 %. At low x values the particle yield shows a dramatic rise when the c.m. energy increases from 5 to 36 GeV. This rise is related to the growth of the multiplicity seen above.

Gluon emission will lead to scale breaking effects: the primary momentum is now shared by quark and gluon resulting in a depletion of particles at high x and an excess of particles at low x values. The effect becomes more pronounced as the energy rises, e.g. the 30 GeV data at $x = 0.2$ are predicted to be higher by ~10%, and at $x = 0.7$ lower by ~20 % than the 5 GeV data[66]. The measurements are not precise enough to test this prediction.

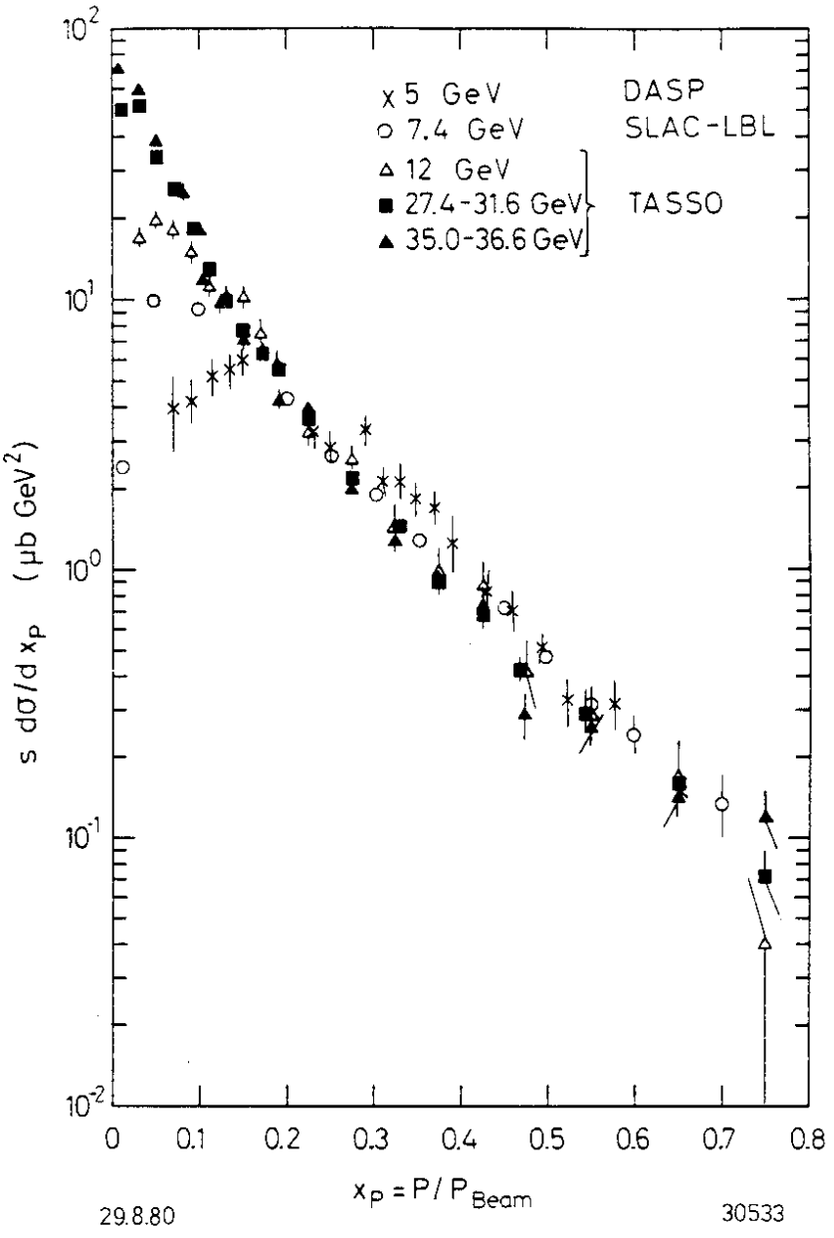

Fig. 27 The scaling cross section $sd\sigma/dx$ ($x=p/E_{beam}$) for inclusive charged particle production measured at energies of 5 GeV (Ref.64), 7.4 GeV (Ref. 65) and between 12 and 36.6 GeV (Ref.62, 63).

11.4 π, K and $p,\bar{p}$ cross sections

Inclusive $\pi^{\pm}$, $K^{\pm}$, K^{0}, $\bar{K}^{0}$, and $p,\bar{p}$ cross sections were measured at PETRA by the experiments listed in Table 3.

Table 3. Experiments measuring particle separated cross sections

type of particle	experiment	technique	momentum range (GeV/c)	remark
$\pi^{\pm}$	JADE	dE/dx [63]	<0.7, 2-7	preliminary
	TASSO	TOF [67]	<1.1	
		Cerenkov [63]	<5	preliminary
$K^{\pm}$	JADE	dE/dx [63]	<0.7	preliminary
	TASSO	TOF [67]	<1.1	
		Cerenkov [63]	<5	preliminary
$K^{0},\overline{K^{0}}$	PLUTO	$K^{0}_{S} \rightarrow \pi^{+}\pi^{-}$ [63]	all P	preliminary
	TASSO	" [68]	"	
$p,\bar{p}$	JADE	dE/dx [63]	<0.9	preliminary
	TASSO	TOF [67]	<2.2	
		Cerenkov [63]	<4	preliminary

Fig. 28 shows the scaling cross section $s/\beta\, d\sigma/dx$ for the sum of $\pi^{+} + \pi^{-}$ production for energies of 5.2 [64], 12 and 30 GeV as a function of $x = 2E/W$. The 12 and 30 GeV points agree with each other but appear to be lower than the 5.2 GeV data by ≈30 % for $x \gtrsim 0.2$. There is a break in slope near $x = 0.1$. The data at lower x values have a larger slope.

In Fig. 29 the same quantity is plotted for $K^{+} + K^{-}$ and $K^{0} + \overline{K^{0}}$ production. Besides the PETRA data at 30 GeV also measurements from 7.4 GeV [69] are shown. For $W = 30$ GeV and $x < 0.1$ where $K^{\pm}$ data are available the $K^{\pm}$ and $K^{0},\overline{K^{0}}$ yields appear to be the same. The K^{0} data indicate a break in slope similar to that seen for the $\pi^{\pm}$ data. The curve in Fig. 29 is a hand drawn average through the high energy $\pi^{\pm}$ data (Fig. 28). The K yield is roughly a factor of 2 to 4 lower than the $\pi^{\pm}$ yield. Towards high x values the difference

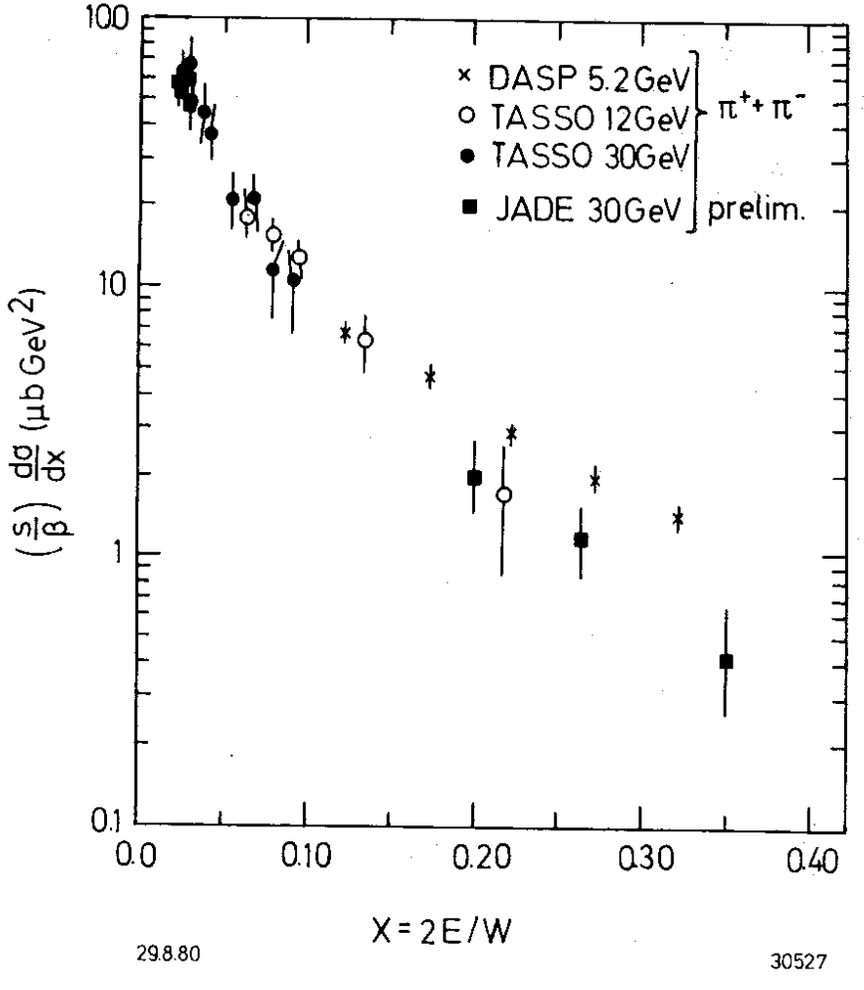

Fig. 28 The cross section $(s/\beta)d\sigma/dx$ $(x=E/E_{beam})$ for the sum of $\pi^+ + \pi^-$ production. (From Ref.63)

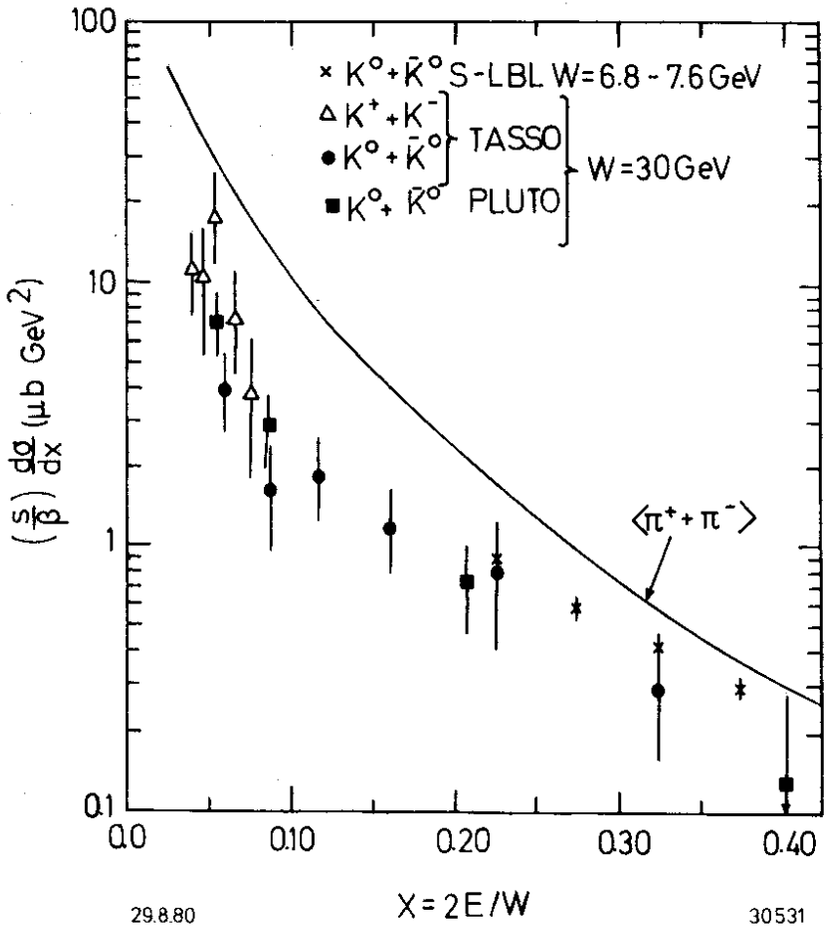

Fig. 29 Same as in Fig. 28 for $K^+ + K^-$ and $K^o + \bar{K}^o$ production. (From Ref.63).

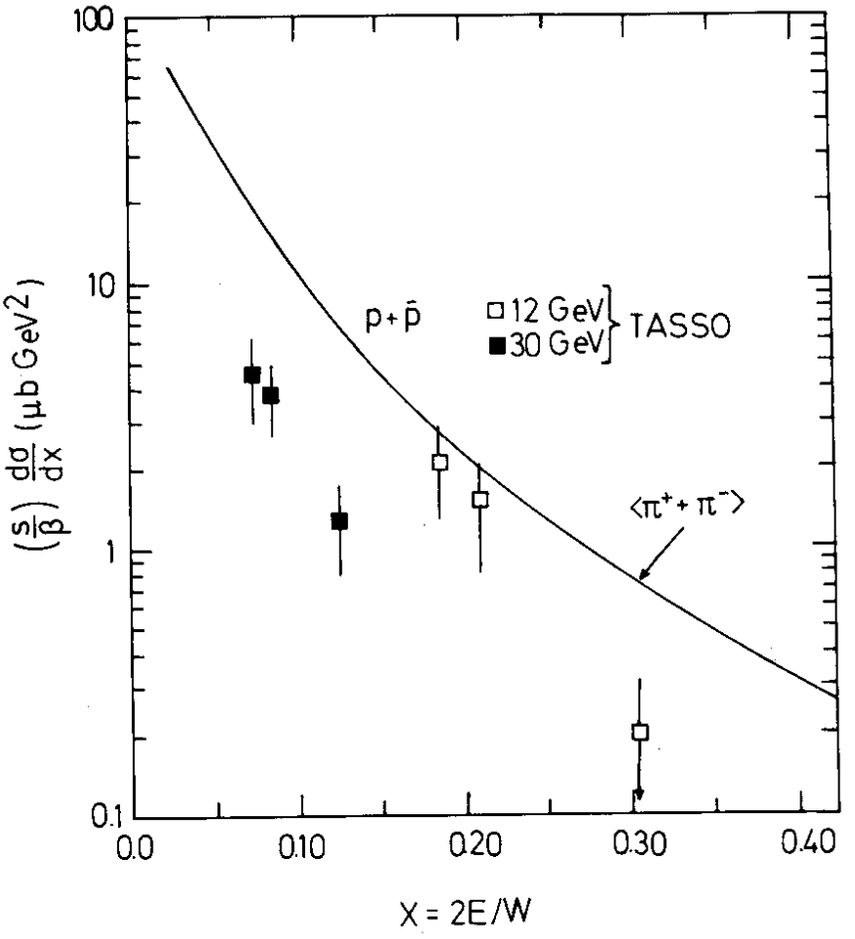

Fig. 30 Same as Fig. 28 for p + $\bar{p}$ production. (From Ref. 63).

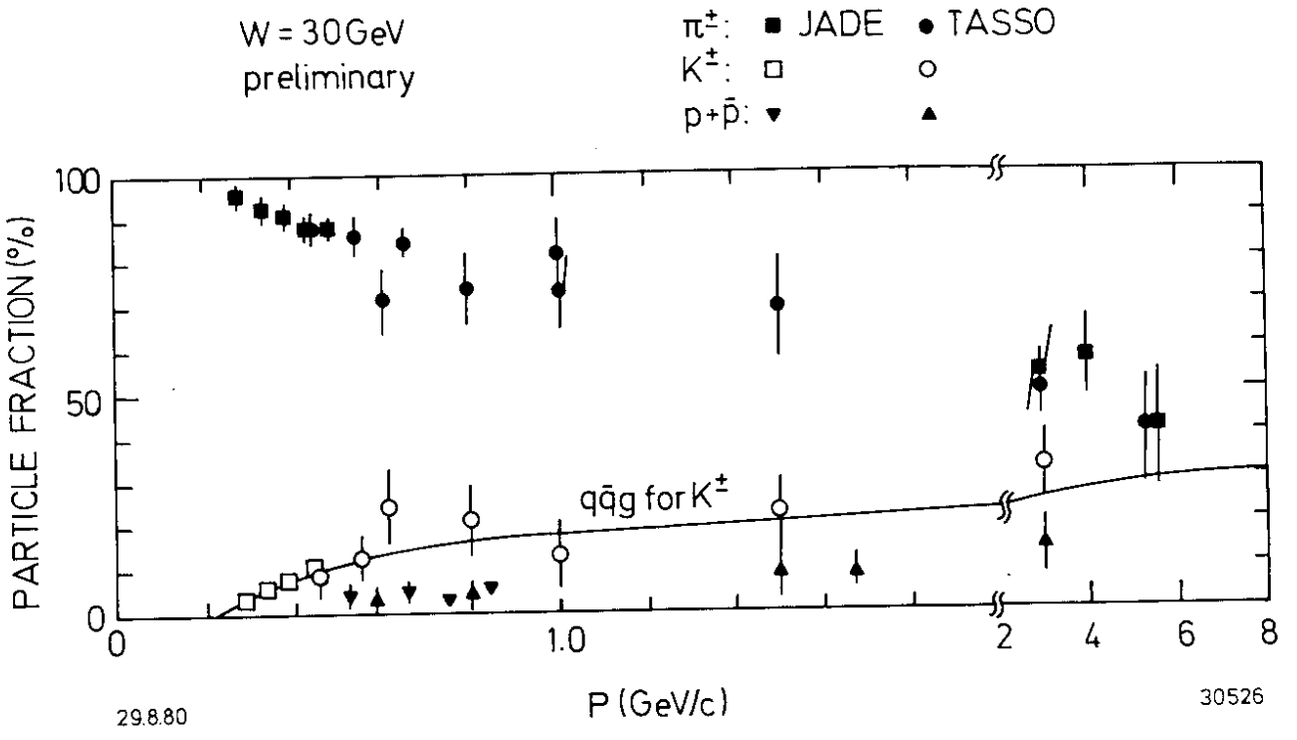

Fig. 31 Charged particle fractions as a function of momentum. (From Ref.63).

becomes smaller, i.e. the π and K yields approach each other.

In Fig. 30 the corresponding data are shown for $p + \bar{p}$ production. The data are rather scanty. The curve shows again the average of the $\pi^{\pm}$ data. Within the large error bars the $K^0,\overline{K^0}$ and the $p,\bar{p}$ yields appear to be the same. This rather large yield for $p,\bar{p}$ seems to be surprising.

Fig. 31 shows the relative fraction of $\pi^{\pm}$, $K^{\pm}$ and $p,\bar{p}$ as a function of particle momentum p at W = 30 GeV. The low momentum particles are basically all pions. As the momentum increases the fractions of $K^{\pm}$ and $p,\bar{p}$ rise, and for $p \approx 4$ GeV/c there seem to be almost as many $K^{\pm}$ as $\pi^{\pm}$. An average event at W = 30 GeV has approximately 11 $\pi^{\pm}$, 1.4 $K^0,\overline{K^0}$, 1.4 $K^{\pm}$ and 0.4 $p,\bar{p}$ in the final state. Assuming that the number of $n,\bar{n}$ equals that of $p,\bar{p}$, out of 5 events two have a baryon antibaryon pair in the final state.
The number of $K^0,\overline{K^0}$ is a factor of 2 - 3 larger than observed in pp final states: at a c.m. energy of 24 GeV there are on the average 0.5 $K^0,\overline{K^0}$ per event[70]. The excess of kaons in e^+e^- annihilation is likely to be due to c and b quark contributions. Hence we may have had a first smell of the primary quark flavours.

12. Summary

The dominant feature of e^+e^- annihilation into hadrons is two jet production with the particle collimation becoming more pronounced as the energy increases. Concurrently with that a new phenomenon shows up at high energies which produces three-jet events. At 30 GeV roughly 5 - 10 % of the events have three distinct jets. The dynamic properties of these events as well as their rate is found to agree with hard gluon bremsstrahlung as predicted by QCD. The strong coupling constant, α_s, deduced from the data at 30 GeV has a value of $0.17 \pm 0.02 \pm 0.3$.

The particle yield at large angles to the jet axes provided a first hint that quark and gluon may fragment differently into hadrons. An attempt was made to measure and interpret the accollinearity distribution between jets. Soft gluon emission combined with the effects of hadronization are able to describe the data.

The final states show a rapidly (in logarithmic terms) rising particle multiplicity above ~7 GeV. This is connected with a strong increase of low momentum particles. The scaling cross sections for pion and kaons possess a similar behaviour. The exponential slope shows a break near x = 0.1. The kaon data - as well as the $p,\bar{p}$ data - lie below the $\pi^{\pm}$ points by a factor of 2-4 depending on x. At high momenta the pion and kaon yields tend to become equal. The large fraction of kaons compared to pp collisions is probably an indication of the different primary quark flavours. The relatively large number of baryons produced in e^+e^- annihilation demands an explanation.

List of References

1. R.F. Schwitters, rapporteur talk, 1975 Stanford Conference, p. 5;
R.F. Schwitters et al., Phys. Rev. Lett. 35 (1975) 1320;
G. Hanson et al., Phys. Rev.Lett. 35 (1975) 1609

2. PLUTO-Collaboration, Ch.Berger et al., Phys. Lett. B78 (1978) 176

3. PLUTO-Collaboration, Ch. Berger et al., Phys. Lett. 82B (1979) 449

4. C.W. Darden et al., Phys. Lett. 80B (1979) 419;
W. Schmidt-Parzefall, 19/8 Tokyo Conference, p. 260

5. J. K. Bienlein et al., Phys. Lett. 78B (1978) 360;
G. Heinzelmann, 1978 Tokyo Conference, p.263

6. PLUTO group, data presented by S. Brand at the 1979 EPS Conference, p.338, and DESY-report 79/41 (1979)

7. K. Koller and T.F. Walsh, Phys. Lett. B72 (1977) 227;
B73 (1978) 5o4 and Nucl. Phys. B140 (1978) 449;
T.A. De Grand et al., Phys. Rev. D16 (1977) 3251;
S.J. Brodsky et al., Phys. Lett. B73 (1978) 2o3

8. K. Koller and H. krasemann, Phys. Lett. 88B (1979) 119

9. B.H. Wiik, Proceedings of the Intern. Neutrino Conference, Bergen, Norway, June 1979, p. 113;
P. Söding, proceedings of the EPS Intern. Conf. on High Energy Phys., Geneva, Switzerland, June-July 1979, p.271
TASSO-Collaboration, R. Brandelik et al., Phys. Lett. 86B (1979) 243

10. MARK J-Collaboration, D.P. Barber et al., Phys. Rev. Lett. 43 (1979) 830

11. PLUTO-Collaboration, Ch. Berger et al., Phys. Lett. 86B (1979) 418

12. JADE-Collaboration, W. Bartel et al., DESY-Report 79/80 (1979)

13. J. Kogut and L. Susskind, Phys. Rev. D9 (1974) 697, 3391
A.M. Polyakov, Proceedings of the 1975 Intern. Symposium on Lepton and Photon Interactions at High Energies, Stanford, Aug. 21-27, 1975
The first discussion on the experimental implications of gluon bremsstrahlung in e^+e^- annihilation was given by:
J. Ellis, M.K. Gaillard and G.G.Ross, Nucl. Phys. B111 (1976), 253
- erratum B 130 (1977) 516
T.A. De Grand, Yee Jack Ng, and S.-H.H. Tye, Phys. Rev. D16(1977) 3251
A. deRujula, J. Ellis,E.G. Floratos and M.K. Gaillard, Nucl. Phys. B138 (1978) 387
G. Kramer and G. Schierholz, Phys. Lett. 82B (1979) 102
G. Kramer, G.Schierholz and J. Willrodt, Phys. Lett. 79B (1978) 249
P. Hoyer, P. Osland, HG.Sander, T.F.Walsh and P.M. Zerwas, DESY 78/21 (1978) to be published
G. Curci, M. Greco and Y. Srivastava, CERN-Report 2632 1979
G. Kramer, G. Schierholz and J. Willrodt, DESY-Report 79/69 (1979)

14. see for example:
G.G. Hanson, 13th Rencontre de Moriond (1978), Vol. II,Gauge Theories and Leptons, edited by J. Tran Thanh Van and SLAC-PUB-2118;

B.H. Wiik and G. Wolf, Electron Positron Interactions, Springer Tracts in Modern Physics, Vol. 86 (1979)
G. Wolf, Lectures given at the 1979 CERN-JINR School, DESY-Report 80/13 (1980)
G. Flügge, Lectures given at the XIII Intern. Winter Meeting of Fund Phys., Spain, KF Karlsruhe Report KFK 2995 (1980)

15. T. Walsh, Talk given at the Vanderbilt Symposium on e^+e^- Interactions, 1980

16. R.D. Field and R.P. Feynman, Nucl. Phys. B136 (1978) 1

17. U. Timm, DESY-Report 80/70 (1980)

18. D. Cords, rapporteur talk at the 1980 Wisconsin Conference

19. D.J. Bjorken and S.J. Brodsky, Phys. Rev. D1 (1970) 1416

20. S. Brandt et al., Phys. Lett. 12 (1964) 57;
E. Fahri, Phys. Rev. Lett. 39 (1977) 1587

21. PLUTO-Collaboration, Ch. Berger et al., Phys. Lett. B78 (1978) 176

22. TASSO-Collaboration, R. Brandelik et al., Z. Physik C4 (1980) 87

23. see e.g. P. Darriulat, CERN Report EP/80-16 (1980), to be published in Ann. Rev. of Nucl. and Particle Science

24. M. Jacob, Lectures given at the 1979 JINR-CERN School

25. TASSO-Collaboration, R. Brandelik et al., Phys. Lett. 86B (1979) 243

26. PLUTO-Collaboration, Ch.Berger et al., Phys. Lett 86 B (1979) 418

27. JADE-Collaboration, W.Bartel et al., Phys. Lett. 91B (1980) 142

28. MARK J-Collaboration, D.P. Barber et al., Phys. Rev. Lett. 43 (1979) 830 and Phys. Lett. 89B (1979) 139

29. S.L. Wu and G. Zobernig, Z. Physik C2 (1979) 107

30. P. Hoyer, P. Osland, H.E.Sander, T.F. Walsh, and P.M. Zerwas, Nucl. Phys. B 616 (1979) 349

31. A. Ali, E. Pietarinen, G. Kramer and J.Willrodt, DESY-Report 79/86 (1979), to be published

32. The Lund Monte Carlo, T. Sjöstrand,B. Söderberg, Lund Report LU TP 78-18 (1978); T. Sjöstrand,Lund Report LU TP-79-8 (1979)

33. R.D.Field and R.P. Feynman, Nucl. Phys. B136 (1978) 1

34. G.Altarelli and G. Parisi, Nucl. Phys. B126 (1977) 298

35. F.A.Berends and R. Kleiss, work to be published

36. MARK-J Collaboration, D.P. Barber et al., Phys. Lett. 89B (1979) 139

37. TASSO-Collaboration, R. Brandelik et al., Phys. Lett. 94B (1980) 437

38. S. Yamada, rapporteur talk at the 1980 Wisconsin Conference

39. V. Hepp, rapporteur talk, ibid.

40. B.Anderson, G. Gustafson, Lund Preprint, LU TP 79-2 (1979)
B.Anderson, G. Gustafson, Z. Physik C 3 (1980) 223
B.Anderson, G. Gustafson, T. Sjöstrand, Lund Report LU TP 80-1 (1980)
B. Anderson, G. Gustafson, C. Peterson, Nucl. Phys. B135 (1978) 273

41. W. Bartel and A. Peterson, DESY-Report 80/46 (1980)
and S. Yamada, Ref. 38

42. Y.L. Dokshitzer, D.I. D'yakanov, S.I. Troyan, Phys. Lett. 78B (1978) 290

43. PLUTO-Collaboration, Ch. Berger et al., Phys. Lett. 90 B (1980) 312

44. F. Halzen and D.M. Scott, Univ. of Hawaii and Univ. of Wisconsin preprint UH-511-379-80/ UW-COO-881-130 (1980)

45. K. Kajantie and E. Pietarinen, DESY-Report 80/19 (1980)

46. R.Baier and K. Fey, Univ. of Bielefeld preprint BI-TP 80/10 (1980)

47. C.L. Basham , L.S. Brown, T.S. Ellis and S.T. Love, Phys. Rev. D17 (1978) 2298, and Phys. Rev. Lett. 41 (1978) 585
K. Konishi, A. Ukawa and G. Veneziano, Phys. Lett. 80B (1979) 259

48. S. Pandoulas, rapporteur talk at the 1980 Wisconcin Conference

49. C.Bacci et al., Phys. Lett. 86B (1979) 234

50. SLAC-LBL Collaboration, G.G. Hanson, 13th Rencontre de Moriond (1978), ed. by J. Tran Thanh Van, Vol. III

51. PLUTO-Collaboration, Ch, Berger et al., Phys. Lett 81B (1979) 410, 78B (1978) 176

52. DASP-Collaboration, R. Brandelik et al., Nucl. Phys. B148 (1979) 189

53. JADE-Collaboration, W.Bartel et al., Phys. Lett. 88B (1979) 171

54. TASSO-Collaboration, R. Brandelik et al., Phys. Lett. 89B (1980) 418

55. PLUTO-Collaboration, Ch. Berger et al., DESY-report 80/69 (1980)

56. W. Thomé et al., Nucl. Phys. B129 (1977) 365; see also the review by E.Albini, P. Capiluppi, G. Giacomelli, and A.M. Rossi, Nuovo Cimento 32A (1976) 101

57. Data given by R. Stenbacka et al., Nuovo Cimento 51A (1979) 63;
see also S. Barshay, A. Fridman and P. Juillot, Phys. Rev. D15 (1977) 2702

58. M. Basile et al., CERN preprint (1980)

59. J. Ellis (private communication), motivated by W. Furmanski, R. Petronzio and S. Pokorski, Nucl. Phys. B155 (1979) 253

60. Z. Koba, H.B. Nielsen and P. Olesen, Nucl. Phys. B40 (1972) 317

61. see e.g. S.D. Drell, D. Levy and T.M. Yan, Phys. Rev. 187 (1969),2159; D1 (197o) 1035, 1617, 2402

62. TASSO-Collaobration, R. Brandelik et al., Phys. Lett. 89B (1980) 418

63. D. Pandoulas, rapporteur talk at the 1980 Wisconsin Conference

64. DASP Collaboration, R. Brandelik et al., Nucl. Phys. B148 (1979) 189

65. G.J. Feldman and M.L. Perl, Physics Reports 33 (1977) 285

66. R.Baier, J. Engels and B. Peterson, University of Bielefeld report BI-TP 79/10 (1979);
W.R. Frazer and J.F. Gunion, Phys. Rev. D20 (1979) 147

67. TASSO-Collaboration, R. Brandelik et al., Phys. Lett. 94B (1980) 444

68. TASSO-Collaboration, R. Brandelik et al., Phys. Lett. 94B (1980) 91

69. V. Lüth et al., Phys. Lett. 70B (1977) 120

70. Dao et al., Phys. Rev. Lett. 30 (1973) 1151
Sheng et al., Phys. Rev. D11 (1975) 1733